

Online Orthogonal Dictionary Learning Based on Frank-Wolfe Method

Ye Xue, *Graduate Student Member, IEEE*, and Vincent LAU, *Fellow, IEEE*

Abstract—Dictionary learning is a widely used unsupervised learning method in signal processing and machine learning. Most existing works of dictionary learning are in an offline manner. There are mainly two offline ways for dictionary learning. One is to do an alternative optimization of both the dictionary and the sparse code; the other way is to optimize the dictionary by restricting it over the orthogonal group. The latter one is called orthogonal dictionary learning which has a lower complexity implementation, hence, it is more favorable for low-cost devices. However, existing schemes on orthogonal dictionary learning only work with batch data and can not be implemented online, which is not applicable for real-time applications. This paper proposes a novel online orthogonal dictionary scheme to dynamically learn the dictionary from streaming data without storing the historical data. The proposed scheme includes a novel problem formulation and an efficient online algorithm design with convergence analysis. In the problem formulation, we relax the orthogonal constraint to enable an efficient online algorithm. In the algorithm design, we propose a new Frank-Wolfe-based online algorithm with a convergence rate of $\mathcal{O}(\ln t/t^{1/4})$. The convergence rate in terms of key system parameters is also derived. Experiments with synthetic data and real-world sensor readings demonstrate the effectiveness and efficiency of the proposed online orthogonal dictionary learning scheme.

Index Terms—online learning, dictionary learning, Frank-Wolfe, sensor, convergence analysis.

I. INTRODUCTION

SPARSE representation of data has been widely used in signal processing, machine learning and data analysis, and shows a highly expressive and effective representation ability [1–5]. It represents the data $\mathbf{y} \in \mathbb{R}^N$ by a linear combination $\mathbf{y} \approx \mathbf{D}^{true} \mathbf{x}$, where $\mathbf{x} \in \mathbb{R}^M$ is a sparse code (i.e., the number of non-zero entries of \mathbf{x} is much smaller than M), and $\mathbf{D}^{true} \in \mathbb{R}^{N \times M}$ is the dictionary that contains the compact information of \mathbf{y} . At the initial stage in this line of research, predefined dictionaries based on Fourier basis and various types of wavelets [6] have been successfully used for processing biomedical images, natural images, and audio signals [3, 7]. However, using the learned dictionary instead of a generic one has been shown to dramatically improve the performance of various tasks, e.g., image denoising [8] and classification [9].

One method to learn the dictionary is to alternatively optimize (AO) problems with both the dictionary and the sparse codes as the variables [1, 10], where the dictionary usually has no constraint. Another way is to restrict the dictionary

over the orthogonal group $\mathbb{O}(N, \mathbb{R})$ and solve the following optimization problem only for the dictionary [11–14]:

$$\underset{\mathbf{D} \in \mathbb{O}(N, \mathbb{R})}{\text{minimize}} \quad \frac{1}{T} \sum_{t=1}^T Sp(\mathbf{D}^T \mathbf{y}_t), \quad (1)$$

where $Sp(\cdot)$ is a sparsity-promoting function. This formulation is motivated by the fact that the sparse code can be obtained as $\{\mathbf{x}_t = (\mathbf{D}^{true})^T \mathbf{D}^{true} \mathbf{x}_t \approx (\mathbf{D}^*)^T \mathbf{y}_t\}_{t=1}^T$ if the dictionary \mathbf{D}^{true} is orthogonal. To process large-scale data, orthogonal dictionary learning (ODL) is more favorable than the AO method for the following reasons. First, ODL has a lower computational complexity. It updates only the dictionary at each iteration, but the AO method requires solving two sub-problems respectively for the dictionary and the sparse code. Second, ODL allows efficient storing and transmitting of the dictionary. In ODL, the $N \times N$ orthogonal dictionary has the degree of freedom $\frac{N(N-1)}{2}$ according to the *submersion theorem* of the manifold [15], hence it can be represented by only $\frac{N(N-1)}{2}$ rotation angles via Givens rotation [16]. The general complete dictionary updated in the AO method, however, need to be presented by N^2 values¹. Third, the ODL has a performance competitive with the AO method in real applications [17], though the orthogonal constraint seemingly brings performance loss as it narrows the optimization space.

However, the existing ODL methods only work with batch data. In other words, they require the whole data set to run the algorithm. Hence, they are not applicable to many of real-time applications, including real-time network monitoring [18], sensor networks [19], and Twitter analysis [20], where data arrives continuously in rapid, unpredictable, and unbounded streams. To deal with the streaming data, we propose an online ODL approach that processes the data in a single sample or in a mini-batch. The online ODL can be regarded as taking $L \rightarrow \infty$ in Problem (1), and is formally formulated as

$$\underset{\mathbf{D} \in \mathbb{O}(N, \mathbb{R})}{\text{minimize}} \quad F(\mathbf{D}) = \mathbb{E}_{\mathbf{y} \sim \mathcal{P}} [Sp(\mathbf{D}^T \mathbf{y})], \quad (2)$$

where \mathbf{y} is the realization of the random variable Y drawn from a distribution \mathcal{P} . Since the distribution \mathcal{P} is usually unknown and the cost of computing the expectation is prohibitive, the main challenge is to solve Problem (2) without the accessibility of $F(\mathbf{D})$ or its gradient $\nabla F(\mathbf{D})$. In this case, we can only rely on the sampled data to calculate the approximation of the objective function or the gradient. These approximations will jeopardize the performance and the convergence of the algorithms compared to the case where the exact objective value and gradient are available [21, 22].

Y. Xue and V. Lau are with the Department of Electronic and Computer Engineering, Hong Kong University of Science and Technology, Hong Kong (E-mail: yxueaf, eeknlau@ust.hk).

¹In the AO method, the dictionary is usually complete or overcomplete. The overcomplete dictionary requires $M \times N (M < N)$ values to represent.

There are many general algorithms for constraint online optimization, such as proximal stochastic gradient descent (ProxSGD) [23], regularized dual averaging (RDA) [24], and stochastic mirror descent (SMD) [25]; however, they cannot be directly applied to Problem (2) due to the nonconvex constraint set and possibly nonconvex sparsity-promoting function, e.g., $\text{Sp}(\cdot) = -\|\cdot\|_p^p$, ($p > 2$) [14, 26, 27]. In this work, to enable an efficient and provable online algorithm, we proposed a novel online ODL solution with a convex relaxation of the orthogonal constraint in Problem (2). After the relaxation, the problem becomes a nonconvex optimization over a convex set. One may solve the relaxed problem by ProxSGD [23]. However, ProxSGD gives rise to two issues: first, the proximal operator [28] in the ProxSGD costs a high per-iteration computational complexity; and second, ProxSGD can only be guaranteed to converge to an ϵ -stationary point when the mini-batch size is increasing by $1/\epsilon$ [23, 29]. To achieve small errors, the mini-batch size needs to be large, which is not suitable for most online processors with limited memories.

To address these issues, we propose a Frank-Wolfe-based [30, 31] algorithm, the Nonconvex Stochastic Frank-Wolfe (NoncvxSFW) method, to solve the relaxed problem with low-complexity per-iteration computation thanks to the linear minimization oracle (LMO) in the Frank-Wolfe method. We also prove that the proposed algorithm with a single sample or a fixed mini-batch size can be guaranteed to converge to a stationary point of the relaxed online ODL problem. The main contributions are summarized as follows.

- **Novel Online ODL Formulation:** We propose an online ODL problem with an ℓ_3 -norm-based sparsity-promoting function and a convex relaxation of the orthogonal constraint. We prove that all the optimal solutions of the original problem are also the optimal solutions of the relaxed problem, which enables an efficient online algorithm with guaranteed convergence.
- **Online Frank-Wolfe-Based Algorithm:** We develop an online algorithm, the NoncvxSFW method, to solve the relaxed optimization problem with a single sample or a fixed mini-batch size. The convergence is analyzed and the convergence rate is shown to be $\mathcal{O}(\ln t/t^{1/4})$, where t is the number of iterations. As far as we are aware, this is the first non-asymptotic convergence rate for online nonconvex optimization using the Frank-Wolfe-based method. The proposed algorithm and the corresponding theoretical results can also be generalized into general online nonconvex problems with convex constraints.
- **Effective and Efficient Application on IoT Sensor Data Compression:** We provide extensive simulations with both synthetic data and a real-world data set. The simulation results demonstrate the effectiveness and efficiency of our proposed online ODL. They also verify the correctness of our theoretical results. For the synthetic data, the proposed scheme can achieve superb performance in terms of the convergence rate and the recovery error. The proposed scheme can achieve a better root mean squared error (RMSE) with a higher compression ratio for the data compression task for IoT sensor readings compared to the

state-of-the-art baselines [14, 32, 33] using a real-world data set.

The rest of the paper is organized as follows. In Section II and III, we illustrate the online ODL scheme and present the problem formulation for the online ODL, respectively. In Section IV, we present the Frank-Wolfe-based online algorithm with non-asymptotic convergence analysis. Numerical simulation results are provided in Section V. Finally, Section VI summarizes the work.

Notations: In this paper, lowercase and uppercase bold face letters stand for column vectors and matrices, respectively. $\mathbb{O}(N, \mathbb{R})$ denotes the N dimensional orthogonal group in the real value field. e_i denotes the standard basis vector with a 1 in the i -th coordinate and 0's elsewhere. The operations $(\cdot)^T$ and $\mathbb{E}[\cdot]$ denote the operations of transpose and expectation, respectively. $\|\cdot\|_p$ is the ℓ_p norm of a vector. For simplicity, the ℓ_2 norm of a vector and the spectral norm of a matrix are denoted by $\|\cdot\|$. \odot denotes the Hadamard product, and $(\cdot)^{\odot p}$ is the element-wise p -th power. $\langle \mathbf{X}, \mathbf{Y} \rangle$ is the general inner product of \mathbf{X} and \mathbf{Y} . $\mathcal{P}_{\mathbb{O}(N, \mathbb{R})}(\mathbf{D})$ projects \mathbf{D} onto the orthogonal group. $\lfloor \cdot \rfloor$ and $\lceil \cdot \rceil$ denotes the floor operator and taking the abstract value. $[a]_b$ denotes that a modulo b . $\mathbf{x} \sim^{i.i.d} \mathcal{BG}(\theta)$ represents that vector \mathbf{x} has i.i.d elements and each is a product of independent Bernoulli and standard normal random variables: $x_i = b_i g_i$, where $b_i \sim \text{Ber}(\theta)$ and $g_i \sim \mathcal{N}(0, 1)$.

II. ONLINE ODL SCHEME

In this section, we introduce the proposed online ODL scheme followed by some real-world application examples.

A. Online ODL Scheme

In the online ODL, we consider that the data samples arrive in streams. At time t , there is one mini-batch of samples $\mathbf{Y}_t = [\mathbf{y}_t^1, \dots, \mathbf{y}_t^{M_t}] \in \mathbb{R}^{N \times M_t}$ arriving at the processor, where M_t is the mini-batch size at time t and \mathbf{y}_t^j is the j -th sample in the t -th mini-batch. Each sample is assumed to be generated by

$$\mathbf{y}_t^j = \mathbf{D}^{true} \mathbf{x}_t^j, \forall j = 1, \dots, M_t, \forall t, \quad (3)$$

where \mathbf{D}^{true} is the orthogonal dictionary and \mathbf{x}_t^j is a realization of the random variable X drawn from some distribution that induces sparsity. The basic goal of the online ODL processor is to dynamically learn the dictionary in an online manner without storing all the historical samples. That is to say, the processor updates the dictionary \mathbf{D}_t at time t only according to the samples arriving at that time, i.e., \mathbf{Y}_t . In the next subsection, we will show that the proposed ODL scheme is a core functional module in many practical applications.

B. Application Examples

In this subsection, we give two important application examples that should adopt the online ODL scheme.

1) *Example 1 (Online Data Compression on Edge Devices in the IoT Network [34, 35]):* Consider the IoT network architecture shown in Fig. 1, where the data are collected from smart objects such as wearables and industrial sensor devices, and are sent periodically to an edge device using short range communication protocols (e.g., WiFi and Bluetooth). The edge device is responsible for low-level processing, filtering, and sending the data to the cloud. We assume that an edge device is

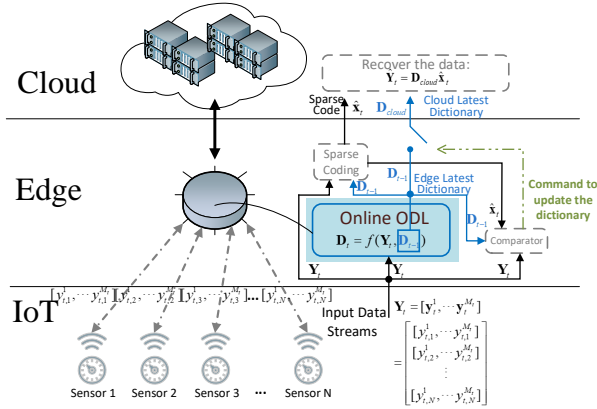


Fig. 1. Illustration of edge data compression in an IoT network using the proposed online ODL scheme.

connected with a total number of N geographically distributed IoT sensors. When sensor measurements (temperature, humidity, concentration, etc.) are required by the cloud from the edge for the data analytics, the edge device transmits a compressed version of the data to save communication resources. At the t -th time slot, the M_t samples of the sensor measurements from all N sensors, $\mathbf{Y}_t = [\mathbf{y}_t^1, \dots, \mathbf{y}_t^{M_t}] \in \mathbb{R}^{N \times M_t}$, are transmitted to an edge device. When the j -th sample from all N sensors, i.e., $\mathbf{y}_t^j, j \in [M_t]$, is required by the cloud, the edge data compression is executed using the following steps:

- 1) *Preprocessing (Sparse Coding on the Edge):* The edge device calculates the sparse code $\hat{\mathbf{x}}_t^j$ based on the *edge latest dictionary* \mathbf{D}_{t-1} and the input \mathbf{y}_t^j .
- 2) *Preprocessing (Transmission Content Decision on the Edge):* Upon obtaining the sparse code $\hat{\mathbf{x}}_t^j$, the edge device calculates the error between \mathbf{y}_t^j and $\mathbf{D}_{cloud} \hat{\mathbf{x}}_t^j$, using a certain error metric $l(\mathbf{y}_t^j, \mathbf{D}_{cloud} \hat{\mathbf{x}}_t^j)$ where \mathbf{D}_{cloud} is a local copy of the *cloud latest dictionary* in the cloud. Then, the edge decides the content to transmit:
 - If the error metric $l(\mathbf{y}_t^j, \mathbf{D}_{cloud} \hat{\mathbf{x}}_t^j)$ is larger than a predetermined threshold, the edge device updates its local cloud dictionary copy as $\mathbf{D}_{cloud} = \mathbf{D}_{t-1}$, and transmits the updated \mathbf{D}_{cloud} to the cloud in the compressed format. It also transmits the sparse code $\hat{\mathbf{x}}_t^j$ to the cloud in a compressed format;
 - Otherwise, the edge only transmits the sparse code $\hat{\mathbf{x}}_t^j$ to the cloud in a compressed format.
- 3) *Core Procedure (Online ODL on the Edge):* The edge device runs the online ODL to produce \mathbf{D}_t using \mathbf{D}_{t-1}

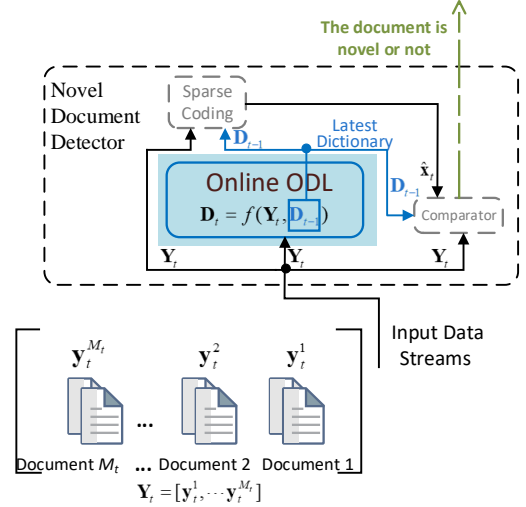


Fig. 2. Illustration of real-time novel document detection using the proposed online ODL scheme.

and the input \mathbf{Y}_t .

- 4) *Postprocessing (Sensor Data Recovery on the Cloud):* The cloud recovers the required data \mathbf{y}_t^j by $\hat{\mathbf{y}}_t^j = \mathbf{D}_{cloud} \hat{\mathbf{x}}_t^j$, where $\hat{\mathbf{x}}_t^j$ is the sparse code received from the edge and \mathbf{D}_{cloud} is the latest dictionary in the cloud.

The proposed ODL module produces the \mathbf{D}_t , \mathbf{D}_{t-1} and \mathbf{D}_{cloud} , which play critical roles in the above example of data compression on the IoT edge devices.

2) *Example 2 (Real-time Novel Document Detection [36, 37]):* Novel document detection can be used to find the breaking news or emerging topics on social media. In this application, $\mathbf{Y}_t = [\mathbf{y}_t^1, \dots, \mathbf{y}_t^{M_t}] \in \mathbb{R}^{N \times M_t}$ denotes the mini-batch of documents arriving at time t , where each column of \mathbf{Y}_t represents a document at that time, as shown in Fig. 2. Each document is represented by some conventional vector space model such as TF-IDF [38]. For the mini-batch of documents \mathbf{Y}_t arriving at time t , the novel document detector operates using the following steps:

- 1) *Preprocessing (Sparse Coding):* For all \mathbf{y}_t^j in \mathbf{Y}_t , calculate the sparse code $\hat{\mathbf{x}}_t^j$ based on the *latest dictionary* \mathbf{D}_{t-1} and the input \mathbf{y}_t^j .
- 2) *Preprocessing (Novel Document Detection):* For all \mathbf{y}_t^j in \mathbf{Y}_t , calculate the error between \mathbf{y}_t^j and $\mathbf{D}_{t-1} \hat{\mathbf{x}}_t^j$ with some error metric $l(\mathbf{y}_t^j, \mathbf{D}_{t-1} \hat{\mathbf{x}}_t^j)$.
 - If the error $l(\mathbf{y}_t^j, \mathbf{D}_{t-1} \hat{\mathbf{x}}_t^j)$ is larger than some pre-defined threshold, mark the document \mathbf{y}_t^j as *novel*;
 - Otherwise, mark the document \mathbf{y}_t^j as *non-novel*.
- 3) *Core Procedure (Online ODL):* Run the online ODL to produce the new dictionary \mathbf{D}_t using \mathbf{D}_{t-1} and the input \mathbf{Y}_t .

III. ONLINE ODL PROBLEM FORMULATION

In this section, we will elaborate on the proposed online ODL problem formulation.

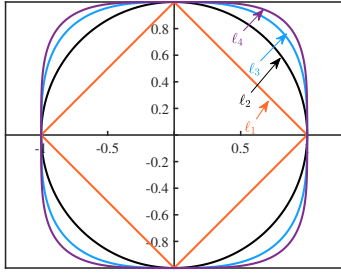


Fig. 3. Unit spheres of the ℓ_p in \mathbb{R}^2 , where $p = 1, 2, 3, 4$. The sparsest points on the unit ℓ_2 -sphere, e.g., points $(0, 1)$, $(0, -1)$, $(1, 0)$ and $(-1, 0)$ in \mathbb{R}^2 , have the largest ℓ_p -norm ($p > 2$).

A. ℓ_3 -Norm-Based Formulation

For the online ODL, the dynamic updating of the dictionary can be done by solving the generic Problem (2) in an online manner. In Problem (2), the sparsity-promoting function $Sp(\cdot)$ needs to be carefully designed since it determines the performance of the online ODL and the complexity of the algorithm. In this work, we use $Sp(\cdot) = -\|\cdot\|_3^3$, which results in the following optimization problem:

$$\underset{\mathbf{D} \in \mathcal{O}(N, \mathbb{R})}{\text{minimize}} \quad F(\mathbf{D}) = \mathbb{E}_{\mathbf{y} \sim \mathcal{P}}[-\|\mathbf{D}^T \mathbf{y}\|_3^3]. \quad (4)$$

The choice of $-\|\cdot\|_3^3$ is inspired by the recent result that minimizing the negative p -th power of the ℓ_p -norm ($p > 2$) with the unit ℓ_2 -norm constraint leads to sparse (or spiky) solutions [14, 26, 39, 40]. An illustration is given in Fig. 3. Compared to the widely used ℓ_1 -norm, the negative ℓ_p -norm formulation allows a convex relaxation of the orthogonal constraint, hence it provides flexibility for the algorithm design, as we will illustrate in Section III-B. Also, the smoothness of this formulation enables a faster convergence of algorithms. In this paper, we choose $p = 3$ since the sample complexity and the total computation complexity achieve the minimum when $p = 3$ among all the choices of p ($p > 2$) for maximizing the ℓ_p -norm over the orthogonal group, as we have proved in [26].

B. Orthogonal Constraint Relaxation

After determining the sparsity-promoting function, to facilitate an efficient online solver with a convergence guarantee, we propose a convex relaxation of the orthogonal constraint in Problem (4) based on the following Lemma.

Lemma 1 ([41, 3.4] Convex Hull of the Orthogonal Group). *The convex hull of the orthogonal group is the (closed) unit spectral ball:*

$$\text{conv}(\mathcal{O}(N, \mathbb{R})) = \mathbb{B}_{sp}(N, \mathbb{R}),$$

where $\mathbb{B}_{sp}(N, \mathbb{R}) := \{\mathbf{X} \in \mathbb{R}^{N \times N} : \|\mathbf{X}\| \leq 1\}$ is the unit spectral ball.

From Lemma 1, we know that the unit spectral ball is the minimal convex set containing the orthogonal group. Then we propose the following relaxed problem for the online ODL:

$$\mathcal{P} : \underset{\mathbf{D} \in \mathbb{B}_{sp}(N, \mathbb{R})}{\text{minimize}} \quad F(\mathbf{D}) = \mathbb{E}_{\mathbf{y} \sim \mathcal{P}}[-\|\mathbf{D}^T \mathbf{y}\|_3^3]. \quad (5)$$

Problem \mathcal{P} is a proper relaxation of Problem (4) since all the optimal solutions of Problem (4) belong to the set of the optimal solutions of Problem \mathcal{P} under some general statistic model for \mathbf{y} . We will show this relationship formally in the following.

We first introduce the following definition of the *sign-permutation matrix* to characterize the optimal solutions,

Definition 1. (*Sign-permutation Matrix*) *The N dimensional sign-permutation matrix $\Xi \in \mathbb{R}^{N \times N}$ is defined as*

$$\Xi = \Sigma \Pi, \quad (6)$$

where $\Sigma = \text{diag}(\pm \mathbf{1}_N)$ with $\mathbf{1}_N$ the N -dimension all one vector, and $\Pi = [e_{\pi(1)}, e_{\pi(2)}, \dots, e_{\pi(N)}]$, with e_n being a standard basis vector and $[\pi(1), \pi(2), \dots, \pi(N)]$ being any permutations of the N elements.

Then, the relationship between the optimal solutions of Problem (4) and Problem \mathcal{P} is formally presented in the following theorem.

Theorem 1 (Consistency of the Relaxation). *If \mathbf{y} follows the distribution \mathcal{P} such that $\mathbf{y} = \mathbf{D}^{true} \mathbf{x}$ with $\mathbf{D}^{true} \in \mathcal{O}(N, \mathbb{R})$ and the entries of \mathbf{x} being i.i.d Bernoulli Gaussian², $\mathbf{x} \sim \text{i.i.d} \mathcal{B}\mathcal{G}(\theta)$. Then the optimal solution of Problem (4) is*

$$\mathbf{D}^{opt} = \mathbf{D}^{true} \Xi^T, \quad (7)$$

which is also an optimal solution of Problem \mathcal{P} . In (7), Ξ is a sign-permutation matrix.

Proof. See Appendix B. \square

Remark 1. *This consistency of the relaxation no longer holds when $-\|\cdot\|_3^3$ in Problem \mathcal{P} is replaced by the widely used sparsity-promoting function $\|\cdot\|_1$. When $\|\cdot\|_1$ is used, the optimal solution over the orthogonal group is still $\mathbf{D}^{true} \Xi^T$ but the optimal solution over the unit spectral ball is $\mathbf{0}$.*

After the convex relaxation, we then focus on solving Problem \mathcal{P} , which is a nonconvex optimization problem over a convex set. The convex set has a key property; it contains the convex combination of any two points in the set. That is to say, if we have $\mathbf{A}, \mathbf{B} \in \mathbb{B}_{sp}(N, \mathbb{R})$, then

$$\eta \mathbf{A} + (1 - \eta) \mathbf{B} \in \mathbb{B}_{sp}(N, \mathbb{R}), \eta \in (0, 1). \quad (8)$$

This property enables an efficient online algorithm with a convergence guarantee, as we will illustrate in the next section.

IV. ONLINE NONCONVEX FRANK-WOLFE-BASED ALGORITHM

In this section, we first outline the proposed Frank-Wolfe-based algorithm, NoncvxSFW, for general online convex-constraint nonconvex problems and then specialize it to solve Problem \mathcal{P} .

²The Bernoulli Gaussian is a typical statistical model for the sparse coefficient, which is widely used for the analysis of dictionary learning [11–14].

A. NoncvxSFW for General Online Non-Convex Optimization

To solve a general online convex-constraint nonconvex problem,

$$\min_{\mathbf{X} \in \underbrace{\mathcal{C}}_{\text{convex}}} F_{gen}(\mathbf{X}) = \mathbb{E}_{\mathbf{y} \sim \mathcal{P}} \left[\underbrace{f(\mathbf{X}, \mathbf{y})}_{\text{nonconvex in } \mathbf{X}} \right], \quad (9)$$

we require the algorithm to have the following properties:

- *Computational Efficiency*: Efficient per-iteration computation.
- *Theoretical Effectiveness*: Theoretical guarantee to convergence to a stationary point.

To fulfill the above properties, we propose NoncvxSFW, as shown in Algorithm 1, which is a variant of the Stochastic Frank-Wolfe method (SFW) in [32]. The SFW method and the corresponding analysis can only be applied to solve convex problems, however, NoncvxSFW and the analysis we proposed in this paper are also capable for nonconvex problems. In the following, we will elaborate on how the proposed NoncvxSFW algorithm satisfies the required properties.

Algorithm 1: NoncvxSFW for General Nonconvex Problem

Data: $\mathbf{Y}_t = [\mathbf{y}_t^1, \dots, \mathbf{y}_t^{M_t}]$

Result: $\{\mathbf{X}_t\}_{t=1}^{\infty}$

Initialization: Averaging weight $\rho_t = 4(t+1)^{-1/2}$, stepsize $\gamma_t = 2(t+2)^{-3/4}$. $\mathbf{G}_0 = \mathbf{0}$ and $\mathbf{X}_0 \in \mathcal{C}$;

for $t = 1, 2, \dots$ **do**

1. Gradient Approximation:

$$\mathbf{G}_t = (1 - \rho_t)\mathbf{G}_{t-1} + \frac{\rho_t}{M_t} \sum_{j \in [M_t]} \nabla f(\mathbf{X}_{t-1}, \mathbf{y}_t^j);$$

2. LMO: $\mathbf{S}_t = \arg \min_{\mathbf{S} \in \mathcal{C}} \langle \mathbf{G}_t, \mathbf{S} \rangle$;

3. Variable Update: $\mathbf{X}_t = \mathcal{P}[(1 - \gamma_t)\mathbf{X}_{t-1} + \gamma_t \mathbf{S}_t]$.

1) *Computational Efficiency for General Non-Convex Optimization*: In Algorithm 1, there are three main steps.

- Step 1 (*Gradient Approximation*) approximates the true gradient $\nabla F_{gen}(\mathbf{X})$ by \mathbf{G}_t in a recursive way. In the calculation, M_t can be fixed along all t . Hence, compared to those methods in [42] and [43] that require an increasing number of stochastic gradient evaluations as the number of iterations t grows, NoncvxSFW is more computationally efficient.
- Step 2 (*LMO*) is a procedure to handle the constraint. It can be regarded as solving a linear approximation of the objective function over the constraint set \mathcal{C} using the approximated gradient produced by Step 1. Compared to the Quadratic Minimization Oracle (QMO) in the projection-based methods, e.g., proximal gradient descent [23], the LMO can be more computationally efficient for many constraint sets, such as the trace norm and the ℓ_p balls [31, 32].
- Step 3 (*Variable Update*) updates the variable \mathbf{X}_t by a simple convex combination of $\mathbf{S}_t \in \mathcal{C}$ and $\mathbf{X}_{t-1} \in \mathcal{C}$, $\mathcal{P}[\mathbf{X}_t = (1 - \gamma_t)\mathbf{X}_{t-1} + \gamma_t \mathbf{S}_t]$, where $\mathcal{P}[\mathbf{X}]$ is any operation that satisfies $\mathcal{P}[\mathbf{X}] \in \mathcal{C}$ and $F_{gen}(\mathcal{P}[\mathbf{X}]) \leq F_{gen}(\mathbf{X})$. According to (8), we have $\mathbf{X}_t = (1 - \gamma_t)\mathbf{X}_{t-1} + \gamma_t \mathbf{S}_t \in \mathcal{C}$. This step only requires the output

from Step 2 and the variable of the last iteration and automatically ensures the feasibility of the output \mathbf{X}_t .

2) *Theoretical Effectiveness for General Non-Convex Optimization*: To show the convergence of the NoncvxSFW, we first introduce the following Frank-Wolfe gap as the measure for the first-order stationary.

Definition 2 (Frank-Wolfe Gap). *The Frank-Wolfe gap at the t -th iteration, g_t^{gen} , is defined as*

$$g_t^{gen} := \max_{\mathbf{S} \in \mathcal{C}} \langle -\nabla F_{gen}(\mathbf{X}_{t-1}), \mathbf{S} - \mathbf{X}_{t-1} \rangle. \quad (10)$$

The Frank-Wolfe gap is a valid first-order stationary measure because of the following Lemma.

Lemma 2 (Frank-Wolfe Gap Is A Measure for Stationarity). *A point \mathbf{X}_{t-1} is a stationary point for the optimization problem (9) if and only if $g_t^{gen} = 0$.*

Proof. See Appendix C. \square

Then we assume the following conditions hold for the general problem (9).

Assumption 1.

- 1) (*Bounded Constraint Set*) *The constraint set \mathcal{C} is bounded with diameter $\text{diam}(\mathcal{C})$ in terms of the Frobenius norm for matrices, i.e.,*

$$\|\mathbf{X} - \mathbf{Y}\|_F \leq \text{diam}(\mathcal{C}), \quad \forall \mathbf{X}, \mathbf{Y} \in \mathcal{C}. \quad (11)$$

- 2) (*Lipschitz Smoothness*) *$F_{gen}(\mathbf{X})$ is L -smooth over the set \mathcal{C} , i.e.,*

$$\|\nabla F_{gen}(\mathbf{X}) - \nabla F_{gen}(\mathbf{Y})\|_F \leq L \|\mathbf{X} - \mathbf{Y}\|_F, \quad \forall \mathbf{X}, \mathbf{Y} \in \mathcal{C}. \quad (12)$$

- 3) (*Unbiased Mini-batch Gradient*) *The mini-batch gradient $\frac{1}{M_t} \sum_{j \in [M_t]} \nabla f(\mathbf{X}_{t-1}, \mathbf{y}_t^j)$ is an unbiased estimation of the true gradient $\nabla F_{gen}(\mathbf{X})$, i.e.,*

$$\mathbb{E} \left[\frac{1}{M_t} \sum_{j \in [M_t]} \nabla f(\mathbf{X}_{t-1}, \mathbf{y}_t^j) \right] = \nabla F_{gen}(\mathbf{X}), \quad \forall t. \quad (13)$$

- 4) (*Bounded Variance of the Mini-batch Gradient*) *The variance of the mini-batch gradient $\frac{1}{M_t} \sum_{j \in [M_t]} \nabla f(\mathbf{X}_{t-1}, \mathbf{y}_t^j)$ is bounded, i.e.,*

$$\mathbb{E} \left[\left\| \frac{1}{M_t} \sum_{j \in [M_t]} \nabla f(\mathbf{X}_{t-1}, \mathbf{y}_t^j) - \nabla F_{gen}(\mathbf{X}) \right\|_F^2 \right] \leq \frac{V}{M_t}, \quad \forall t. \quad (14)$$

The above assumptions ensure the convergence of NoncvxSFW, which is formally stated in the following Theorem.

Theorem 2 (Convergence of NoncvxSFW for the General Nonconvex Problem). *If the conditions in Assumption 1 hold, using Algorithm 1 to solve the general problem (9), we have that the expected Frank-Wolfe gap converges to zero, in a sense that*

$$\begin{aligned} & \inf_{1 < s \leq t} \mathbb{E} \left[g_s^{gen} \right] \\ & \leq \frac{c_1 (\sqrt{\max\{C_0, C_1^t\}} \text{diam}(\mathcal{C}) + L \text{diam}(\mathcal{C})^2) \ln(t+2)}{(t+3)^{\frac{1}{4}}}, \end{aligned} \quad (15)$$

where $C_0 = \|\nabla F_{gen}(\mathbf{X}_0)\|_F^2$, $C_1^t = \frac{4V}{\min\{M_t\}} + 2L^2 \text{diam}(\mathcal{C})^2$ and c_1 is some positive constant. In other words, Algorithm 1 is guaranteed to converge to a stationary point of the general problem (9) at a rate of $\mathcal{O}(\ln(t)/t^{1/4})$ in expectation.

Proof. See Appendix D. \square

The above convergence result holds for the general online convex constraint nonconvex problems.

B. NoncvxSFW for the Proposed Online ODL Problem

In this section, we will apply the proposed NoncvxSFW to solve the proposed online ODL Problem \mathcal{P} . The algorithm is summarized in Algorithm 2. Similar to Section IV-A, we will

Algorithm 2: NoncvxSFW for the proposed Online ODL

Data: $\mathbf{Y}_t = [\mathbf{y}_t^1, \dots, \mathbf{y}_t^{M_t}]$

Result: $\{\mathbf{D}_t\}_{t=1}^\infty$

Initialization: Averaging weight $\rho_t = 4(t+1)^{-1/2}$, stepsize $\gamma_t = 2(t+2)^{-3/4}$. $\mathbf{G}_0 = \mathbf{0}$ and $\mathbf{D}_0 \in \mathbb{B}_{sp}(N, \mathbb{R})$;

for $t = 1, 2, \dots$ **do**

1. Gradient Approximation:

$$\mathbf{G}_t = (1 - \rho_t)\mathbf{G}_{t-1} + \frac{\rho_t}{M_t} \sum_{j \in [M_t]} -\nabla \|\mathbf{D}^T \mathbf{y}_t^j\|_3^3;$$

2. LMO: $\mathbf{U}, \mathbf{\Sigma}, \mathbf{V}^T = \text{SVD}(-\mathbf{G}_t)$;

$$\mathbf{S}_t = \mathbf{U}\mathbf{V}^T;$$

3. Variable Update:

$$\mathbf{D}_t = \text{Polar}((1 - \gamma_t)\mathbf{D}_{t-1} + \gamma_t \mathbf{S}_t).$$

illustrate the NoncvxSFW for the proposed Online ODL from the computational and theoretical aspects.

1) *Computational Efficiency for the Proposed Online ODL Problem:* When adopting NoncvxSFW for Problem \mathcal{P} , Step 1 remains unchanged in Algorithm 1. Step 2 (LMO) is calculated based on the following Lemma.

Lemma 3 (LMO for the Unit Spectral Ball). *The minimum value of $\langle \mathbf{G}, \mathbf{S} \rangle, \forall \mathbf{S} \in \mathbb{B}_{sp}(N, \mathbb{R})$ is the nuclear norm of $-\mathbf{G}$, i.e.,*

$$\min_{\mathbf{S} \in \mathbb{B}_{sp}(N, \mathbb{R})} \langle \mathbf{G}, \mathbf{S} \rangle = \|-\mathbf{G}\|_*. \quad (16)$$

The minimum is achieved when \mathbf{S} belongs to the subdifferential of $\|-\mathbf{G}\|_$, i.e.,*

$$\mathbf{S}^* = \arg \min_{\mathbf{S} \in \mathbb{B}_{sp}(N, \mathbb{R})} \langle \mathbf{G}, \mathbf{S} \rangle = \mathbf{U}\mathbf{V}^T \in \partial \|-\mathbf{G}\|_*, \quad (17)$$

where $\mathbf{U}, \mathbf{\Sigma}, \mathbf{V}^T = \text{SVD}(-\mathbf{G})$.

Proof. The proof can be done by simply using the definition of the dual norm and the subdifferential of norm $\|\cdot\|_*$. \square

Using the LMO to deal with the constraint is much more computationally friendly than the QMO used in the projection-based method. In the QMO, the proximal operator for the

matrix spectral norm requires a proximal operator for the ℓ_∞ -norm of the singular vector, which has no closed-form solution [44].

In Step 3, the polar decomposition is adopted inspired by [45, Proposition 3.4]. The following lemma shows that it is a valid specification of \mathcal{P} in Algorithm 1.

Lemma 4. (Validation of Variable Update Step) *Let $\mathbf{X} \in \mathbb{B}_{sp}(N, \mathbb{R})$, then we have $\text{Polar}(\mathbf{X}) \in \mathbb{B}_{sp}(N, \mathbb{R})$ and $F(\text{Polar}(\mathbf{X})) \leq F(\mathbf{X})$.*

Proof. See Appendix E. \square

2) *Theoretical Effectiveness for the Proposed Online ODL Problem:* In this subsection, we will adapt the convergence theory in Theorem 2 to the proposed online ODL problem. We first show in the following Lemma that the conditions in Assumption 1 are satisfied by Problem \mathcal{P} .

Lemma 5 (The ODL Problem Satisfies the Convergence Condition). *If \mathbf{y} follows the distribution \mathcal{P} such that for all t and all j , $\mathbf{y}_t^j = \mathbf{D}^{true} \mathbf{x}_t^j$ with $\mathbf{D}^{true} \in \mathbb{O}(N, \mathbb{R})$ and the entries of \mathbf{x}_t^j being i.i.d Bernoulli Gaussian, $\mathbf{x}_t \sim^{i.i.d} \mathcal{BG}(\theta)$, then Problem \mathcal{P} satisfies the conditions in Assumption 1. Specifically, we have*

1) (Bounded Constraint Set)

$$\|\mathbf{D}_1 - \mathbf{D}_2\|_F \leq \sqrt{2N}, \forall \mathbf{D}_1, \mathbf{D}_2 \in \mathbb{B}_{sp}(N, \mathbb{R}). \quad (18)$$

2) (Lipschitz Smoothness) $F(\mathbf{D})$ is L -smooth over the set $\mathbb{B}_{sp}(N, \mathbb{R})$, i.e.,

$$\|\nabla F(\mathbf{D}_1) - \nabla F(\mathbf{D}_2)\|_F \leq \sqrt{\frac{2}{\pi}} N^{3/2} (N+1) \theta \|\mathbf{D}_1 - \mathbf{D}_2\|_F, \quad \forall \mathbf{D}_1, \mathbf{D}_2 \in \mathbb{B}_{sp}(N, \mathbb{R}). \quad (19)$$

3) (Unbiased Mini-batch Gradient) *The mini-batch gradient $\frac{1}{M_t} \sum_{j \in [M_t]} -\nabla \|\mathbf{D}^T \mathbf{y}_t^j\|_3^3$ is an unbiased estimation of the true gradient $\nabla F(\mathbf{D})$, i.e.,*

$$\mathbb{E} \left[\frac{1}{M_t} \sum_{j \in [M_t]} -\nabla \|\mathbf{D}^T \mathbf{y}_t^j\|_3^3 \right] = \nabla F(\mathbf{D}), \quad \forall t. \quad (20)$$

4) (Bounded Variance of the Mini-batch Gradient) *The variance of the mini-batch gradient $\frac{1}{M_t} \sum_{j \in [M_t]} -\nabla \|\mathbf{D}^T \mathbf{y}_t^j\|_3^3$ is bounded, i.e., for all t , we have*

$$\mathbb{E} \left[\left\| \frac{1}{M_t} \sum_{j \in [M_t]} -\nabla \|\mathbf{D}^T \mathbf{y}_t^j\|_3^3 - \nabla F(\mathbf{D}) \right\|_F^2 \right] \leq \frac{3\theta N^2}{M_t}. \quad (21)$$

Proof. See Appendix F. \square

Based on Lemma 5 and Theorem 2, we have the convergence result for Algorithm 2, as shown in the following Theorem.

Theorem 3 (Convergence of NoncvxSFW for the Proposed Online ODL Problem). *Using Algorithm 2 to solve Problem \mathcal{P} , we have that the expected Frank-Wolfe gap*

$$\mathbb{E} [g_t] := \mathbb{E} \left[\max_{\mathbf{S} \in \mathbb{B}_{sp}(N, \mathbb{R})} \langle -\nabla F(\mathbf{D}_{t-1}), \mathbf{S} - \mathbf{D}_{t-1} \rangle \right]$$

³The detailed deduction can be found in <https://stephentu.github.io/blog/convex-analysis/2014/10/01/subdifferential-of-a-norm.html>.

converges to zero, in a sense that

$$\begin{aligned} & \inf_{1 < s \leq t} \mathbb{E} [g_s] \\ & \leq \frac{c_2 \left(\sqrt{C_0 N + \frac{\theta N^3}{\min\{M_t\}} + \theta^2 N^5 (N+1)^2 + \theta N^{\frac{5}{2}} (N+1)} \right) \ln(t+2)}{(t+3)^{\frac{1}{4}}}, \end{aligned} \quad (22)$$

where $C_0 = \|\nabla F(\mathbf{D}_0)\|_F^2$, and c_2 is a positive constant.

Proof. Proof can be done by substituting the results in Lemma 5 into Theorem 2. \square

Remark 2 (Impact of the Key System Parameters). *Theorem 3 suggests that a larger number of the smallest mini-batch size $\min\{M_t\}$, a smaller number of dictionary size N , and a smaller sparsity level θ (data becomes more sparse with a smaller θ) will lead to a faster convergence rate. These conclusions are consistent with the simulation results in Section V-B. Though the above theorem only proves the convergence to stationary points, we have observed in experiments that the algorithm actually converges to the global optimum under very broad conditions, as shown in section Section V-B. Similar phenomena also appeared in many other works on offline ODL [11, 13, 14, 26].*

V. EXPERIMENTS

This section provides experiments demonstrating the effectiveness and the efficiency of our scheme compared to the state-of-the-art prior works. All the experiments are conducted in Python 3.7 with a 3.6 GHz Intel Core I7 processor.

A. List of Baseline Methods

The baseline methods are listed as follows:

- **Baseline 1** (SFW) [32]: This baseline is a recently proposed SFW method for solving the *convex* problems which can be implemented online. We compare the proposed NoncvxSFW to this baseline in terms of the convergence property to show the effectiveness and efficiency of the proposed NoncvxSFW method for solving the online ODL problem.
- **Baseline 2** (ℓ_4 -NoncvxSFW) [14]: In this baseline, we replace the sparsity-promoting function, $-\|\cdot\|_3^3$ in the ODL problem \mathcal{P} by $-\|\cdot\|_4^4$. Then, we solve the problem by the NoncvxSFW algorithm. This baseline is to demonstrate the advantage of the proposed online ODL formulation.
- **Baseline 3** (Online AODL) [33]: This baseline alternatively solves the following optimization problem in an online manner:

$$\underset{\mathbf{D} \in \mathbb{R}^{N \times N}, \{\mathbf{x}_t \in \mathbb{R}^N\}_{t=1}^T}{\text{minimize}} \sum_{t=1}^T \|\mathbf{y}_t - \mathbf{D}\mathbf{x}_t\|_F^2 + \lambda \|\mathbf{x}_t\|_1. \quad (23)$$

The online AODL is introduced to show the advantage of the online ODL scheme. The Python SPAMS toolbox is used to implement this baseline.⁴

⁴Python code and documents are available on <http://spams-devel.gforge.inria.fr/downloads.html>.

B. Experiments with Synthetic Data

1) *Experiment Settings:* For all synthetic experiments, we generate the measurements $\mathbf{y}_t^j = \mathbf{D}_{true} \mathbf{x}_t^j$ ($j \in [M_t], 1 \leq t \leq L$), with the ground truth dictionary \mathbf{D}_{true} drawn uniformly randomly from the orthogonal group $\mathbb{O}(N)$, and with sparse signals $\mathbf{x}_t^j \in \mathbb{R}^N$ drawn from i.i.d. Bernoulli-Gaussian distribution $\mathbf{x}_t^j \sim^{i.i.d.} \mathcal{BG}(\theta)$. Without loss of generality, we set $M_t = B$, $\forall t$ and $L = 3 \times 10^3$ for data generation. All the results in this subsection are conducted by averaging over 100 Monte Carlo trials.

2) *Convergence Comparison with Different System Parameters:* To evaluate the convergence property, we use the Error metric as in [14] and [26] for the ODL problem, which is defined as

$$\text{Error}_t = \left| 1 - \frac{\|\mathbf{D}_t^T \mathbf{D}_{true}\|_4^4}{N} \right|, \quad (24)$$

at the t -th iteration. This metric is a measure for the *global optimality* of the ODL problem \mathcal{P} since Theorem 1 shows that a perfect dictionary recovery gives $\frac{\|\mathbf{D}_t^T \mathbf{D}_{true}\|_4^4}{N} = 1$. We compare the *textError* _{t} versus the number of iterations of the proposed NoncvxSFW method and of the baseline methods in the following plots.

In Fig. 4, we show the convergence properties under different mini-batch sizes B with a fixed dictionary size $N = 10$ and sparsity level $\theta = 0.3$. The result shows a larger mini-batch size B that can accelerate the convergence of all methods, and the proposed NoncvxSFW can converge to an error at 10^{-3} with around 1000 iterations, which is faster than the baselines.

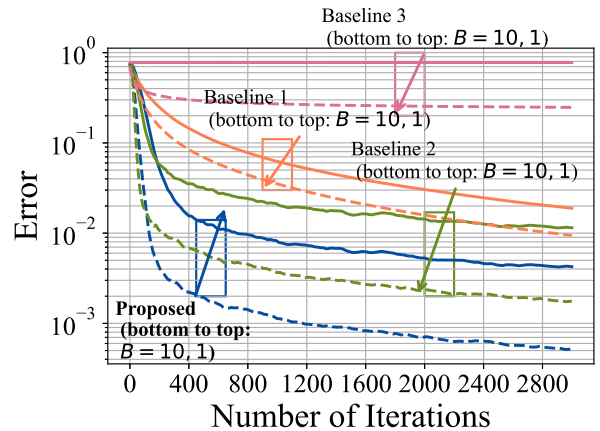


Fig. 4. Convergence comparison under different mini-batch sizes B with dictionary size $N = 10$ and sparsity level $\theta = 0.3$.

In Fig. 5, the convergence curves with different dictionary sizes N are plotted. We fix the mini-batch size to be $B = 10$ and the sparsity level to be $\theta = 0.3$. The result shows that all the methods have a faster convergence rate under a smaller dictionary size N . In addition, the proposed NoncvxSFW is more robust to a larger dictionary size and has a faster convergence rate than the baselines.

In Fig. 6, we compare the convergence properties with different sparsity levels θ . The mini-batch size and the dictionary size are fixed at $B = 10$ and $N = 10$. The result shows that

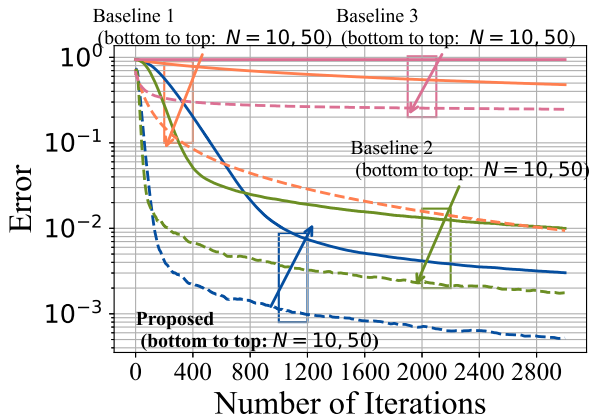


Fig. 5. Convergence comparison under different dictionary size N with mini-batch size $B = 10$, sparsity level $\theta = 0.3$.

both the proposed NoncvxSFW and the baselines have a faster convergence rate with a more sparse \mathbf{x} (smaller θ). Moreover, the proposed NoncvxSFW shows a faster convergence rate than the baselines.

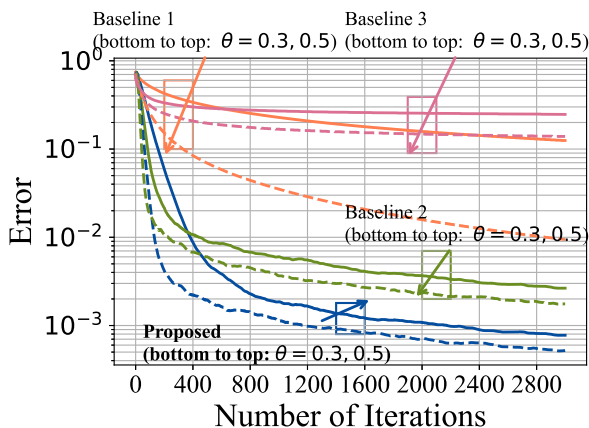


Fig. 6. Convergence comparison under different sparsity levels θ with dictionary size $N = 10$ and mini-batch size $B = 10$.

C. Experiments with a Real-World Sensor Data Set

1) Experiment Settings:

- Experiment Data Set:** We evaluate the performance of the online data compression task with different online dictionary learning methods. The experiments are carried out on the *Airly network air quality data set* [46], which records temperature, air pressure, humidity, and the concentrations of particulate matter from Jan. 1, 2017 to Dec. 25, 2017 generated by a network of $N = 56$ low-cost sensors located in Krakow, Poland. Each sensor has its own location⁵. There are 8593 readings for each item from each sensor sampled per hour. In this work, we use the *temperature readings* from all the sensors as the input to the online dictionary learning schemes. Since there is

⁵Detailed location information with latitude and longitude can be found in the dataset [46].

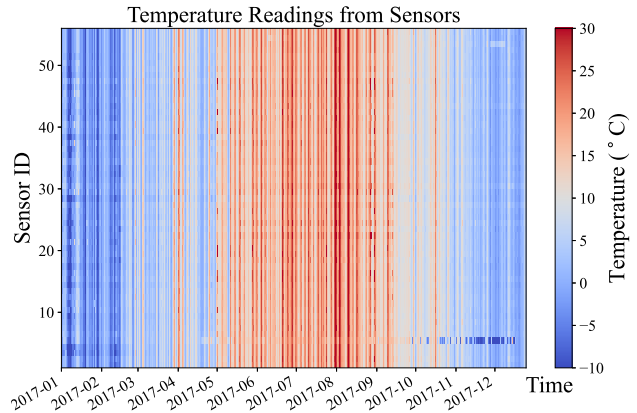


Fig. 7. 56×8593 temperature readings from the *Airly network air quality data set* [46]. The readings are from a sensor network with 56 sensors deployed in different locations in Krakow, Poland. The readings are collected every hour from Jan 1, 2017 to Dec. 25, 2017.

TABLE I
EXPERIMENT PARAMETERS

Parameters	Value
Number of Sensors (dictionary size)	$N = 56$
Total Number of Samples	$\sum_{t=0}^T M_t = 8500$
Initial Batch Size	$M_0 = 100$
Initial Number of Iterations	20
Online Mini-batch Size	$M_t = 6, \forall t = 1 \dots T$
Total Number of Mini-batches	$T = 1400$

a missing data issue in the raw data, we replace those missing data by the mean readings over all the sensors at the time when data is missing. Fig. 7 displays the temperature readings that the online dictionary learning schemes process.

• Experiment Procedures:

- (Initialization):** We use the first M_0 temperature readings to initialize the dictionary \mathbf{D}_0 by the batch version of each scheme.
- (Online Learning):** We run different online dictionary learning schemes with the t -th mini-batch readings to produce \mathbf{D}_t .
- (Online Compression):** We compress each reading in the mini-batch by the sparse code at each iteration after obtaining the dictionary \mathbf{D}_t .

- For Baseline 2 and the proposed method, the sparse code for the j -th sample \mathbf{y}_t^j is calculated using

$$\tilde{\mathbf{x}}_t^j = \mathcal{T}_{\eta_0}(\mathbf{D}_t^T \mathbf{y}_t^j),$$

where $\mathcal{T}_{\eta_0}(\mathbf{a})$ selects η_0 elements in \mathbf{a} with the largest ℓ_2 -norm and sets the other elements to zero.

- For Baseline 3, since there is no orthogonal restriction of the dictionary, the sparse code is

$$\tilde{\mathbf{x}}_t^j = \mathcal{T}_{\eta_0}(\arg \min \|\mathbf{y}_t^j - \mathbf{D}_t \mathbf{x}\|_F^2 + \lambda \|\mathbf{x}\|_1).$$

- (Recovery Error Calculation):** Then, the RMSEs for different schemes are compared under different

TABLE II
RMSE AND PER-ITERATION CPU TIME COMPARISON

Settings	Proposed		Baseline 2 (ℓ_4 -NoncvxSFW)		Baseline 3 (Online AODL)	
	RMSE	CPU Time (ms)	RMSE	CPU Time (ms)	RMSE	CPU Time (ms)
28 ($\eta_0 = 2$)	5.34%	0.8769	5.50%	0.8895	87.54%	3.301
18 ($\eta_0 = 3$)	4.43%	0.8772	4.55%	0.8898	87.40%	3.306
14 ($\eta_0 = 4$)	4.00%	0.8773	4.13%	0.8901	87.39%	3.311
11 ($\eta_0 = 5$)	3.72%	0.8774	3.85%	0.8906	87.33%	3.312
9 ($\eta_0 = 6$)	3.50%	0.8775	3.62%	0.8907	87.31%	3.314
8 ($\eta_0 = 7$)	3.30%	0.8785	3.43%	0.8932	87.30%	3.315
7 ($\eta_0 = 8$)	3.13%	0.8793	3.25%	0.8941	87.26%	3.315
6 ($\eta_0 = 9$)	2.97%	0.8798	3.09%	0.8950	87.24%	3.317
5 ($\eta_0 = 10$)	2.83%	0.8801	2.95%	0.8958	87.19%	3.321
4 ($\eta_0 = 13$)	2.44%	0.8831	2.56%	0.8982	87.18%	3.322
3 ($\eta_0 = 17$)	2.01%	0.8856	2.13%	0.9002	87.10%	3.325
2 ($\eta_0 = 25$)	1.33%	0.8890	1.46%	0.9047	86.98%	3.330
1 ($\eta_0 = 35$)	0.71%	0.8911	0.91%	0.9082	86.90%	3.343

compression ratios. RMSE and compression ratio are defined as

$$\text{RMSE} = \sqrt{\frac{\sum_{t=0}^T \sum_{j=1}^{M_t} \|\mathbf{D}_t \tilde{\mathbf{x}}_t^j - \mathbf{y}_t^j\|_2^2}{\sum_{t=0}^T \sum_{j=1}^{M_t} \|\mathbf{y}_t^j\|_2^2}},$$

$$\text{compression ratio} = \left\lfloor \frac{56}{\eta_0} \right\rfloor.$$

- **Experiment Parameters:** The parameter settings are listed in Table.I.

2) *Performance Comparison:* The RMSE and CPU time comparison among different online dictionary learning schemes under different compression ratios are given in Table II. The results demonstrate that the online ODL scheme achieves a much lower RMSE for the data compression task than the online AODL and requires less computational resources. Furthermore, ℓ_3 -based online ODL shows a slightly better performance in both RMSE and the CPU time than the ℓ_4 -based scheme.

VI. CONCLUSION

We have proposed in this paper a novel online orthogonal dictionary learning scheme with a new relaxed problem formulation, the Frank-Wolfe-based online algorithm, and the convergence analysis. Experiments on synthetic data and the real-world data set show the superior performance of our proposed scheme to the baselines and verify the correctness of our theoretical results. There are many potential directions for future work, e.g., extending the current online scheme into a distributed scheme and combining it with real-world physical impairments to develop an application-specific solution.

APPENDIX A AUXILIARY LEMMAS

Lemma 6. Let $\langle \mathbf{A}, \mathbf{B} \rangle$ be the Frobenius inner product of real matrices $\mathbf{A} \in \mathbb{R}^{N \times M}$ and $\mathbf{B} \in \mathbb{R}^{N \times M}$, then we have for any $\epsilon > 0$

$$\langle \mathbf{A}, \mathbf{B} \rangle \leq \frac{\epsilon^p}{p} \|\text{vec}(\mathbf{A})\|_p^p + \frac{\epsilon^{-q}}{q} \|\text{vec}(\mathbf{B})\|_q^q. \quad (25)$$

Proof. According to the definition of the Frobenius norm, we have

$$\begin{aligned} \langle \mathbf{A}, \mathbf{B} \rangle &= \text{vec}(\mathbf{A})^T \text{vec}(\mathbf{B}) = \sum_{i=1}^M \sum_{j=1}^N A_{j,i} B_{j,i} \\ &= \sum_{i=1}^M \sum_{j=1}^N \epsilon A_{j,i} \epsilon^{-1} B_{j,i} \leq \sum_{i=1}^M \sum_{j=1}^N \left(\frac{\epsilon^p}{p} A_{j,i}^p + \frac{\epsilon^{-q}}{q} B_{j,i}^q \right), \end{aligned} \quad (26)$$

where the last inequality is according to Young's Inequality [47]. \square

Lemma 7. Let $f(s)$ be any decreasing function of s . We have

$$\int_{\mu=a}^{b+1} f(\mu) d\mu \leq \sum_{s=a}^b f(s) \leq \int_{\mu=a-1}^b f(\mu) d\mu. \quad (27)$$

APPENDIX B PROOF THEOREM 1

Let $\mathbf{W} = \mathbf{D}^T \mathbf{D}^{true} \in \mathbb{R}^{N \times N}$, we have

$$\begin{aligned} \mathbb{E}_{\mathbf{y} \sim \mathcal{BG}(\theta)} [-\|\mathbf{D}^T \mathbf{y}\|_3^3] &= - \sum_{n=1}^{n=N} \mathbb{E}[\|\mathbf{W}_{n,:} \mathbf{x}\|_3^3] \\ &= - \sum_{n=1}^{n=N} \mathbb{E}[\|(\mathbf{W}_{n,:} \odot \mathbf{b}^T) \mathbf{g}\|_3^3], \end{aligned} \quad (28)$$

where we denote $\mathbf{b} \sim_{i.i.d} \mathbb{B}_{sp}(\theta)$ and $\mathbf{g} \sim_{i.i.d} \mathcal{CN}(0, 1)$. Using the rotation-invariant property of Gaussian random variables, we have $-\mathbb{E}[\|\mathbf{W}_{n,:} \odot \mathbf{b}^T \mathbf{g}\|_3^3] = -\gamma_1 \mathbb{E}[\|\mathbf{W}_{n,:} \odot \mathbf{b}^T\|_3^3]$ with $\gamma_1 = \frac{2^{3/2}}{\sqrt{\pi}}$ calculated by the 3rd-order non-central moment of the Gaussian distribution.

For Problem (4), we have $\mathbf{D} \in \mathcal{O}(N, \mathbb{R})$ and $\|\mathbf{W}_{n,:}\|_2 = \|\mathbf{D}_{:,n}^T \mathbf{D}^{true}\|_2 \leq 1$. Hence, we have $0 \leq \mathbb{E}[\|\mathbf{W}_{n,:} \odot \mathbf{b}^T\|_2^2] \leq \mathbb{E}[\|\mathbf{W}_{n,:} \odot \mathbf{b}^T\|_2^2] = \theta$. The equality holds if and only if $\|\mathbf{W}_{n,:} \odot \mathbf{b}^T\|_2 \in \{0, 1\}$ for all \mathbf{b} , which is only satisfied at $\mathbf{W}_{n,:} \in \{\pm \mathbf{e}_i^T : i \in [N]\}$ [13]. Therefore, we have $\mathbb{E}_{\mathbf{y} \sim \mathcal{BG}(\theta)} [-\|\mathbf{D}^T \mathbf{y}\|_3^3] = - \sum_{n=1}^{n=N} \mathbb{E}[\|\mathbf{W}_{n,:} \odot \mathbf{b}^T\|_3^3] \geq -N\gamma_1\theta$ and the minimum is achieved when $\mathbf{W}_{n,:} \in$

$\{\pm e_i^T : i \in [N]\}$. Furthermore, if $\mathbf{W}_{n_1,:} = \pm e_i^T$ and $\mathbf{W}_{n_2,:} = \pm e_i^T$, then $\text{Tr}(\mathbf{W}_{n_1,:} \mathbf{W}_{n_2,:}^T) = 1$. However, we have $\text{Tr}(\mathbf{W}_{n_1,:} \mathbf{W}_{n_2,:}^T) = \text{Tr}((\mathbf{D}_{:,n_1}^T \mathbf{D}^{true}) (\mathbf{D}_{:,n_2}^T \mathbf{D}^{true})^T) = \text{Tr}(\mathbf{D}_{:,n_1}^T \mathbf{D}_{:,n_2}) = 0$. This indicates that two different columns of \mathbf{W} cannot simultaneously equal the same standard basis vector. Hence, $\mathbb{E}_{\mathbf{y} \sim \mathcal{BG}(\theta)}[-\|\mathbf{D}^T \mathbf{y}\|_3^3]$ achieves the minimum $-N\gamma_1\theta$ when $\mathbf{D} = \mathbf{D}^{opt}$ with $(\mathbf{D}^{opt})^T \mathbf{D}^{true} = \mathbf{\Xi}$. In other words, the optimal solution of Problem (4) is $\mathbf{D}^{opt} = \mathbf{D}^{true} \mathbf{\Xi}^T$.

For Problem \mathcal{P} , we have $\mathbf{D} \in \mathbb{B}_{sp}(N, \mathbb{R})$, but $\|\mathbf{W}_{n,:}\|_2 = \|\mathbf{D}_{:,n}^T \mathbf{D}^{true}\|_2 \leq 1$ still holds. Hence, we also have $\mathbb{E}_{\mathbf{y} \sim \mathcal{BG}(\theta)}[-\|\mathbf{D}^T \mathbf{y}\|_3^3] = -\sum_{n=1}^N \mathbb{E}[\|\mathbf{W}_{n,:} \odot \mathbf{b}^T\|_2^3] \geq -N\gamma_1\theta$ and the minimum is achieved when $\mathbf{W}_{n,:} \in \{\pm e_i^T : i \in [N]\}$. Since $\mathbf{D}^{opt} = \mathbf{D}^{true} \mathbf{\Xi}^T \in \mathbb{B}_{sp}(N, \mathbb{R})$ is feasible for Problem \mathcal{P} , \mathbf{D}^{opt} is also an optimal solution for Problem \mathcal{P} .

APPENDIX C PROOF OF LEMMA 2

The definition of the stationary points for a constraint problem is

Definition 3 (Definition of Stationary Points). *We will say that $\mathbf{X}^* \in \mathcal{C}$ is a stationary point if*

$$\langle \nabla F_{gen}(\mathbf{X}^*), \mathbf{S} - \mathbf{X}^* \rangle \geq 0, \forall \mathbf{S} \in \mathcal{C}.$$

Then, we first show the sufficient condition. If $g_t^{gen} = 0$, we have

$$\min_{\mathbf{S} \in \mathcal{C}} \langle \nabla F_{gen}(\mathbf{X}_{t-1}), \mathbf{S} - \mathbf{X}_{t-1} \rangle = 0.$$

According to Definition 3, obviously \mathbf{X}_{t-1} is a stationary point.

Next, we show the necessary condition. If $\langle \nabla F_{gen}(\mathbf{X}_{t-1}), \mathbf{S} - \mathbf{X}_{t-1} \rangle \geq 0, \forall \mathbf{S} \in \mathcal{C}$, then we have

$$\langle -\nabla F_{gen}(\mathbf{X}_{t-1}), \mathbf{S} - \mathbf{X}_{t-1} \rangle \leq 0, \forall \mathbf{S} \in \mathcal{C}, \quad (29)$$

which indicates

$$\max_{\mathbf{S} \in \mathcal{C}} \langle -\nabla F_{gen}(\mathbf{X}_{t-1}), \mathbf{S} - \mathbf{X}_{t-1} \rangle = g_t^{gen} \leq 0. \quad (30)$$

Let $\mathbf{S}^* = \arg \max_{\mathbf{S} \in \mathcal{C}} \langle -\nabla F_{gen}(\mathbf{X}_{t-1}), \mathbf{S} \rangle$, then we have $g_t^{gen} = \langle -\nabla F_{gen}(\mathbf{X}_{t-1}), \mathbf{S}^* - \mathbf{X}_{t-1} \rangle \geq 0$. Combining the result in (30), we have that if $\langle \nabla F_{gen}(\mathbf{X}_{t-1}), \mathbf{S} - \mathbf{X}_{t-1} \rangle \geq 0, \forall \mathbf{S} \in \mathcal{C}$, then $g_t^{gen} = 0$.

The sufficient and necessary conditions complete the proof.

APPENDIX D PROOF OF THEOREM 2

For simplicity, we let $F(\cdot)$ represent $F_{gen}(\cdot)$. To prove Theorem 2, we first prove the *Iterates Contraction* by the following Lemma.

Lemma 8 (Iterates Contraction). *Under Assumptions 1, the Frank-Wolfe gap for Problem (9) using Algorithm (1) satisfies*

$$\gamma_t g_t^{gen} \leq F(\mathbf{X}_t) - F(\mathbf{X}_{t+1}) + \gamma_t \sqrt{\epsilon_t} \text{diam}(\mathcal{C}) + \frac{L}{2} \gamma_t^2 N \text{diam}(\mathcal{C})^2, \quad (31)$$

where N is the dimension of the subspace that \mathcal{C} belongs to and

$$\epsilon_t := \|\mathbf{G}_t - \nabla F(\mathbf{X}_{t-1})\|_F^2 \quad (32)$$

is the gradient estimation error.

Proof. We introduce the auxiliary variable

$$\mathbf{S}_t^* := \arg \max_{\mathbf{S} \in \mathcal{C}} \langle -\nabla F(\mathbf{X}_{t-1}), \mathbf{S} \rangle \quad (33)$$

for the proof. At the t -th iteration, we have

$$\begin{aligned} F(\mathbf{X}_t) &\leq F(\mathbf{X}_{t-1} + \gamma_t(\mathbf{S}_t - \mathbf{X}_{t-1})) \\ &\stackrel{(a)}{\leq} F(\mathbf{X}_{t-1}) + \gamma_t \langle \nabla F(\mathbf{X}_{t-1}), \mathbf{S}_t - \mathbf{X}_{t-1} \rangle \\ &\quad + \frac{L\gamma_t^2}{2} \|\mathbf{S}_t - \mathbf{X}_{t-1}\|_F^2 \\ &\stackrel{(b)}{\leq} F(\mathbf{X}_{t-1}) + \gamma_t \langle \mathbf{G}_t, \mathbf{S}_t^* - \mathbf{X}_{t-1} \rangle + \frac{L\gamma_t^2}{2} \|\mathbf{S}_t - \mathbf{X}_{t-1}\|_F^2 \\ &\quad + \gamma_t \langle \nabla F(\mathbf{X}_{t-1}) - \mathbf{G}_t, \mathbf{S}_t - \mathbf{X}_{t-1} \rangle \\ &= F(\mathbf{X}_{t-1}) + \gamma_t \langle \nabla F(\mathbf{X}_{t-1}) - \mathbf{G}_t, \mathbf{S}_t - \mathbf{S}_t^* \rangle \\ &\quad + \gamma_t \langle \nabla F(\mathbf{X}_{t-1}), \mathbf{S}_t^* - \mathbf{X}_{t-1} \rangle + \frac{L\gamma_t^2}{2} \|\mathbf{S}_t - \mathbf{X}_{t-1}\|_F^2 \\ &\stackrel{(c)}{\leq} F(\mathbf{X}_{t-1}) + \gamma_t \|\nabla F(\mathbf{X}_{t-1}) - \mathbf{G}_t\|_F \|\mathbf{S}_t - \mathbf{S}_t^*\|_F \\ &\quad - \gamma_t g_t^{gen} + \frac{L\gamma_t^2}{2} \|\mathbf{S}_t - \mathbf{X}_{t-1}\|_F^2 \\ &= F(\mathbf{X}_{t-1}) + \gamma_t \sqrt{\epsilon_t} \text{diam}(\mathcal{C}) - \gamma_t g_t + \frac{L\gamma_t^2}{2} \text{diam}(\mathcal{C})^2 \\ &\Rightarrow \gamma_t g_t \leq F(\mathbf{X}_{t-1}) - F(\mathbf{X}_t) + \gamma_t \sqrt{\epsilon_t} \text{diam}(\mathcal{C}) \\ &\quad + \frac{L}{2} \gamma_t^2 \text{diam}(\mathcal{C})^2, \end{aligned} \quad (34)$$

where (a) is from Assumption 1, (b) is from Algorithm (1), and (c) is from the Cauchy-Schwarz inequality. \square

The next key ingredient for the proof is the diminishing gradient estimation error as formally shown in the following Lemma.

Lemma 9 (Diminishing Gradient Estimation Error). *Let the gradient estimation error at the t -th iteration in Algorithm (1) defined as*

$$\epsilon_t := \|\mathbf{G}_t - \nabla F(\mathbf{X}_{t-1})\|_F^2. \quad (35)$$

Using the updating rule of Algorithm (1), we have

$$\mathbb{E}[\epsilon_t] \leq \frac{\max\{C_0, C_1^t\}}{(t+2)^{1/2}}, \quad (36)$$

where $C_0 = \|\nabla F(\mathbf{X}_0)\|_F^2$, and $C_1^t = \frac{16V}{M_t} + 2L^2 \text{diam}(\mathcal{C})^2$.

Proof. To prove Lemma 9 we have the following bound with \mathbb{E}_t the conditional expectation w.r.t. the randomness sampled

at the t -th iteration, conditioned on all randomness up to the t -th iteration.

$$\begin{aligned}
 & \mathbb{E}_t[\|\mathbf{G}_t - \nabla F(\mathbf{X}_{t-1})\|_F^2] \\
 = & \mathbb{E}_t[\|(1 - \rho_t)\mathbf{G}_{t-1} + \frac{\rho_t}{|M_t|} \sum_{i \in M_t} \nabla f(\mathbf{X}_{t-1}, \mathbf{y}_i) - \nabla F(\mathbf{X}_{t-1})\|_F^2] \\
 = & \mathbb{E}_t[\|\rho_t(\nabla F(\mathbf{X}_{t-1}) - \mathbf{G}_{t-1}) - \frac{1}{|M_t|} \sum_{i \in M_t} \nabla f(\mathbf{X}_{t-1}, \mathbf{y}_i) \\
 & + (1 - \rho_t)(\nabla F(\mathbf{X}_{t-1}) - \mathbf{G}_{t-1})\|_F^2] \\
 = & \mathbb{E}_t[\|\rho_t(\nabla F(\mathbf{X}_{t-1}) - \frac{1}{|M_t|} \sum_{i \in M_t} \nabla f(\mathbf{X}_{t-1}, \mathbf{y}_i)) \\
 & + (1 - \rho_t)(\nabla F(\mathbf{X}_{t-1}) - \nabla F(\mathbf{X}_{t-2})) \\
 & + (1 - \rho_t)(\nabla F(\mathbf{X}_{t-2}) - \mathbf{G}_{t-1})\|_F^2] \tag{37}
 \end{aligned}$$

$$\begin{aligned}
 (37) = & \rho_t^2 \mathbb{E}_t[\|\nabla F(\mathbf{X}_{t-1}) - \frac{1}{|M_t|} \sum_{i \in M_t} \nabla f(\mathbf{X}_{t-1}, \mathbf{y}_i)\|_F^2 \\
 & + (1 - \rho_t)^2 \|\nabla F(\mathbf{X}_{t-1}) - \nabla F(\mathbf{X}_{t-2})\|_F^2 \\
 & + (1 - \rho_t)^2 \|\nabla F(\mathbf{X}_{t-2}) - \mathbf{G}_{t-1}\|_F^2 \\
 & + 2\rho_t(1 - \rho_t) \mathbb{E}_t[\langle \nabla F(\mathbf{X}_{t-1}) \\
 & - \frac{1}{|M_t|} \sum_{i \in M_t} \nabla f(\mathbf{X}_{t-1}, \mathbf{y}_i), \nabla F(\mathbf{X}_{t-1}) - \nabla F(\mathbf{X}_{t-2}) \rangle] \\
 & + 2\rho_t(1 - \rho_t) \mathbb{E}_t[\langle \nabla F(\mathbf{X}_{t-1}) \\
 & - \frac{1}{|M_t|} \sum_{i \in M_t} \nabla f(\mathbf{X}_{t-1}, \mathbf{y}_i), \nabla F(\mathbf{X}_{t-2}) - \mathbf{G}_{t-1} \rangle] \\
 & + 2(1 - \rho_t)^2 \langle \nabla F(\mathbf{X}_{t-1}) - \nabla F(\mathbf{X}_{t-2}), \nabla F(\mathbf{X}_{t-2}) - \mathbf{G}_{t-1} \rangle \mathbb{E}[\gamma_t g_t^{gen}] \leq \mathbb{E}[F(\mathbf{X}_{t-1}) - F(\mathbf{X}_t)] + \gamma_t \sqrt{\mathbb{E}[\epsilon_t]} \text{diam}(\mathcal{C}) \tag{38}
 \end{aligned}$$

$$\begin{aligned}
 (38) = & \rho_t^2 \mathbb{E}_t[\|\nabla F(\mathbf{X}_{t-1}) - \frac{1}{|M_t|} \sum_{i \in M_t} \nabla f(\mathbf{X}_{t-1}, \mathbf{y}_i)\|_F^2 \\
 & + (1 - \rho_t)^2 \|\nabla F(\mathbf{X}_{t-1}) - \nabla F(\mathbf{X}_{t-2})\|_F^2 \\
 & + (1 - \rho_t)^2 \|\nabla F(\mathbf{X}_{t-2}) - \mathbf{G}_{t-1}\|_F^2 \\
 & + 2(1 - \rho_t)^2 \langle \nabla F(\mathbf{X}_{t-1}) - \nabla F(\mathbf{X}_{t-2}), \nabla F(\mathbf{X}_{t-2}) - \mathbf{G}_{t-1} \rangle \\
 & \stackrel{(a)}{\leq} \rho_t^2 \frac{V}{|M_t|} + (1 - \rho_t)^2 \|\nabla F(\mathbf{X}_{t-1}) - \nabla F(\mathbf{X}_{t-2})\|_F^2 \\
 & + (1 - \rho_t)^2 \|\nabla F(\mathbf{X}_{t-2}) - \mathbf{G}_{t-1}\|_F^2 \\
 & + 2(1 - \rho_t)^2 \langle \nabla F(\mathbf{X}_{t-1}) - \nabla F(\mathbf{X}_{t-2}), \nabla F(\mathbf{X}_{t-2}) - \mathbf{G}_{t-1} \rangle \tag{39}
 \end{aligned}$$

$$\begin{aligned}
 (38) \stackrel{(b)}{\leq} & \rho_t^2 \frac{V}{|M_t|} + (1 - \rho_t)^2 \|\nabla F(\mathbf{X}_{t-1}) - \nabla F(\mathbf{X}_{t-2})\|_F^2 \\
 & + (1 - \rho_t)^2 \|\nabla F(\mathbf{X}_{t-2}) - \mathbf{G}_{t-1}\|_F^2 \\
 & + (1 - \rho_t)^2 \left(\frac{2}{\rho_t} \|\nabla F(\mathbf{X}_{t-1}) - \nabla F(\mathbf{X}_{t-2})\|_F \right. \\
 & \left. + \frac{\rho_t}{2} \|\nabla F(\mathbf{X}_{t-2}) - \mathbf{G}_{t-1}\|_F \right) \\
 \stackrel{(c)}{\leq} & \rho_t^2 \frac{V}{|M_t|} + (1 - \rho_t)^2 \left(1 + \frac{2}{\rho_t}\right) \gamma_{t-1}^2 L^2 \text{diam}(\mathcal{C})^2 \\
 & + (1 - \rho_t)^2 \left(1 + \frac{\rho_t}{2}\right) \|\nabla F(\mathbf{X}_{t-2}) - \mathbf{G}_{t-1}\|_F^2 \\
 \stackrel{(d)}{\leq} & \rho_t^2 \frac{V}{|M_t|} + \frac{2}{\rho_t} \gamma_{t-1}^2 L^2 \text{diam}(\mathcal{C})^2 \\
 & + (1 - \frac{\rho_t}{2}) \|\nabla F(\mathbf{X}_{t-2}) - \mathbf{G}_{t-1}\|_F^2, \tag{40}
 \end{aligned}$$

where (a) is obtained using Assumption 1, (b) is according to Lemma 6 with $\epsilon = \frac{\rho_t}{2}$ and $p = q = 2$, and (c) is obtained from

$$\begin{aligned}
 \|\nabla F(\mathbf{X}_t) - \nabla F(\mathbf{X}_{t-1})\|_F^2 & \leq L^2 \|\mathbf{X}_t - \mathbf{X}_{t-1}\|_F^2 \\
 = L^2 \gamma_t^2 \|\mathbf{S}_t - \mathbf{X}_{t-1}\|_F^2 & \leq L^2 \gamma_t^2 \text{diam}(\mathcal{C})^2 \tag{41}
 \end{aligned}$$

via Assumption (1) and Algorithm (1). In (d), we use the inequality $(1 - \rho_t)^2(1 + \frac{2}{\rho_t}) \leq (1 - \rho_t)(1 + \frac{2}{\rho_t}) \leq \frac{2}{\rho_t}$ and $(1 - \rho_t)^2(1 + \frac{\rho_t}{2}) \leq (1 - \rho_t)(1 + \frac{\rho_t}{2}) \leq (1 - \frac{\rho_t}{\rho_t})$.

Therefore, we have

$$\begin{aligned}
 \mathbb{E}_t[\epsilon_t] & \leq (1 - \frac{\rho_t}{2}) \|\mathbf{G}_{t-1} - \nabla F(\mathbf{X}_{t-2})\|_F^2 \\
 & + \frac{2L^2 \text{diam}(\mathcal{C})^2 \gamma_t^2}{\rho_t} + \rho_t^2 \frac{V}{M_t}, \tag{42}
 \end{aligned}$$

and

$$\begin{aligned}
 \mathbb{E}[\epsilon_t] & = \mathbb{E}_{0,1,\dots,t}[\epsilon_t] \\
 & \leq (1 - \frac{4(t+1)^{-1/2}}{2}) \mathbb{E}_{0,1,\dots,t-1}[\epsilon_{t-1}] \\
 & + (2L^2 \text{diam}(\mathcal{C})^2 + 16 \frac{V}{M_t}) (\eta_0 + t)^{-1}. \tag{43}
 \end{aligned}$$

Then, using the result in [48, Lemma 17], we have finished the proof. \square

We are now able to prove Theorem 2. Based on Lemma 8, Lemma 9, and Jensen's inequality, we have

$$\begin{aligned}
 \mathbb{E}[F(\mathbf{X}_{t-1}) - F(\mathbf{X}_t)] & + \gamma_t \sqrt{\mathbb{E}[\epsilon_t]} \text{diam}(\mathcal{C}) \\
 & + \frac{L}{2} \gamma_t^2 \text{diam}(\mathcal{C})^2. \tag{44}
 \end{aligned}$$

Define $C_* = \max F(\mathbf{X}) - \min F(\mathbf{X})$, we have

$$\begin{aligned}
 \inf_{1 \leq s \leq t} \mathbb{E}[g_s] \sum_{s=1}^t \gamma_s & \leq C_* + \sum_{s=1}^t (\gamma_s \sqrt{\frac{\max\{C_0, C_1^t\}}{(s + \eta_0 + 1)^{1/2}} \text{diam}(\mathcal{C})} \\
 & + \frac{L}{2} \gamma_s^2 \text{diam}(\mathcal{C})^2). \tag{45}
 \end{aligned}$$

Hence, we have

$$\begin{aligned}
 \inf_{1 \leq s \leq t} \mathbb{E}[g_s] & \leq \left(C_* + \sum_{s=1}^t (\gamma_s \sqrt{\frac{\max\{C_0, C_1^t\}}{(s + \eta_0 + 1)^{1/2}} \text{diam}(\mathcal{C})} \right. \\
 & \left. + \frac{L}{2} \gamma_s^2 \text{diam}(\mathcal{C})^2) \right) / \left(\sum_{s=1}^t \gamma_s \right) \\
 & \leq \left(C_* + \sum_{s=1}^t (2(s+2)^{-1} \sqrt{\max\{C_0, C_1^t\}} \text{diam}(\mathcal{C}) \right. \\
 & \left. + \frac{L}{2} 4(s+2)^{-3/2} \text{diam}(\mathcal{C})^2) \right) / \left(\sum_{s=1}^t 2(s+2)^{-3/4} \right) \\
 & \leq \left(C_* + \sum_{s=1}^t ((s+2)^{-1} (2\sqrt{\max\{C_0, C_1^t\}} \text{diam}(\mathcal{C}) \right. \\
 & \left. + 2L \text{diam}(\mathcal{C})^2) \right) / \left(\sum_{s=1}^t 2(s+2)^{-3/4} \right) \tag{46}
 \end{aligned}$$

Since both $(s+2)^{-1}$ and $(s+2)^{-3/4}$ are decreasing in terms of s , from Lemma 7, we have

$$\sum_{s=1}^t (s+2)^{-1} \leq \ln(2+t) - \ln(2), \quad (47)$$

and

$$\sum_{s=1}^t (s+2)^{-3/4} \geq 4((t+3)^{1/4} - 3^{1/4}) \geq \frac{2}{5}(t+3)^{1/4}, \quad \forall s > 1. \quad (48)$$

Hence, we have

$$\begin{aligned} \inf_{1 \leq s \leq t} \mathbb{E}[g_s] &\leq 5 \left(C_* + 10(\ln(2+t) - \ln(2)) \right. \\ &\quad \times \left. (\sqrt{\max\{C_0, C_1\}} \text{diam}(\mathcal{C}) + L \text{diam}(\mathcal{C})^2) \right) \\ &\quad / \left(4(t+3)^{1/4} \right) \\ &\leq \left(5C_* + 10 \ln(t+2) (\sqrt{\max\{C_0, C_1\}} \text{diam}(\mathcal{C}) \right. \\ &\quad \left. + L \text{diam}(\mathcal{C})^2) \right) / \left(4(t+3)^{1/4} \right). \end{aligned} \quad (49)$$

This finishes the proof.

APPENDIX E PROOF OF LEMMA 4

Since $\text{Polar}(\mathbf{D}) \in \mathbb{O}(N, \mathbb{R})$ for $\mathbf{D} \in \mathbb{B}_{sp}(N, \mathbb{R})$, we know that $\mathbb{B}_{sp}(N, \mathbb{R})$ from Lemma 1.

Define $\text{Polar}(\mathbf{D})$ as \mathbf{D}^O . Let $\mathbf{W} = \mathbf{D}^T \mathbf{D}_{true}$ and $\mathbf{W}^O = (\mathbf{D}^O)^T \mathbf{D}_{true}$. It is easy to know that \mathbf{W}^O has orthonormal rows while rows of \mathbf{W}^O lie in the unit ball. Using similar calculations as in Eq.(28) and the discussion below, we have

$$-\sum_{n=1}^N \mathbb{E}[\|\mathbf{W}_{n,:}^O \odot \mathbf{b}^T\|_2^3] \leq -\sum_{n=1}^N \mathbb{E}[\|\mathbf{W}_{n,:} \odot \mathbf{b}^T\|_2^3]. \quad (50)$$

Hence, we have $F(\text{Polar}(\mathbf{D})) \leq F(\mathbf{D})$ from Eq.(28). This completes the proof.

APPENDIX F PROOF OF LEMMA 5

We first show condition (1) is satisfied. $\forall \mathbf{D}_1, \mathbf{D}_2 \in \mathbb{B}_{sp}(N, \mathbb{R})$, we have

$$\begin{aligned} \|\mathbf{D}_1 - \mathbf{D}_2\|_F &= \sqrt{\text{trace}((\mathbf{D}_1 - \mathbf{D}_2)^T (\mathbf{D}_1 - \mathbf{D}_2))} \\ &\leq \sqrt{\text{trace}(\mathbf{D}_1^T \mathbf{D}_1 + \mathbf{D}_2^T \mathbf{D}_2)} \leq \sqrt{N + N} = \sqrt{2N}. \end{aligned} \quad (51)$$

For condition (2), we define $\mathbf{d} = \text{vec}(\mathbf{D})$ and $f_v(\mathbf{d}) = f_v(\text{vec}(\mathbf{D})) = \nabla F(\mathbf{D}) = \nabla \mathbb{E}_{\mathbf{y} \sim \mathcal{P}}[-\|\mathbf{D}^T \mathbf{y}\|_3^3]$. Since we have $\|\mathbf{D}_1 - \mathbf{D}_2\|_2 = \|\mathbf{d}_1 - \mathbf{d}_2\|_2$, the following holds

$$\begin{aligned} \|\nabla f_v(\mathbf{d}_1) - \nabla f_v(\mathbf{d}_2)\|_2 &\leq \|\mathbf{D}_a[f_v(\mathbf{d}_1)]\| \|\mathbf{d}_1 - \mathbf{d}_2\|_2 \\ &\leq \|\mathbf{D}_a[f_v(\mathbf{d}_1)]\|_F \|\mathbf{d}_1 - \mathbf{d}_2\|_2 \\ &= \sqrt{\sum_{i=1}^{N^2} \sum_{j=1}^{N^2} \mathbf{D}_a[f_v(\mathbf{d}_1)]_{i,j} \|\mathbf{d}_1 - \mathbf{d}_2\|_2}, \end{aligned} \quad (52)$$

where $\mathbf{D}_a[f_v(\mathbf{d})]$ is the differential of $f_v(\mathbf{d})$ in terms of \mathbf{d} . To prove condition (2), we only need to show that

$$\sqrt{\sum_{i=1}^{N^2} \sum_{j=1}^{N^2} (\mathbf{D}_a[f_v(\mathbf{d}_1)]_{i,j})^2} \leq \sqrt{\frac{2}{\pi}} N^{3/2} (N+1) \theta. \quad (53)$$

Letting $\mathbf{W} = \mathbf{D}_1^T \mathbf{D}_{true}$ and using the strategy in [13, B.1], we have the j -th element of $f_v(\mathbf{d}_1)$ being

$$f_v(\mathbf{d}_1)_j = \mathbb{E}_\Omega \left[\mathbf{D}_{true([j]-N,:)} (\|\mathbf{W}_{(\lceil \frac{j}{N} \rceil, :)}^\Omega\| \|\mathbf{W}_{(\lceil \frac{j}{N} \rceil, :)}^\Omega)\|^T \right], \quad (54)$$

where Ω is used to denote the generic support set of the Bernoulli random viable contained in \mathbf{x} with $\mathbf{y} = \mathbf{D}_{true} \mathbf{x}$. Then, we have the i, j -th element in $\mathbf{D}_a[f_v(\mathbf{d}_1)]$ as

$$\left(\mathbf{D}_a[f_v(\mathbf{d}_1)]_{i,j} \right)^2 \begin{cases} \leq \left(\mathbb{E}_\Omega [N \|\mathbf{W}_{(\lceil \frac{j}{N} \rceil, :)}^\Omega\| + \|\mathbf{W}_{(\lceil \frac{j}{N} \rceil, :)}^\Omega\|] \right)^2, \\ \text{if } N(\lceil \frac{j}{N} \rceil - 1) + 1 \leq i \leq N(\lceil \frac{j}{N} \rceil) \\ = 0, \text{ otherwise.} \end{cases} \quad (55)$$

From [26, B.1], we know that

$$\mathbb{E}_\Omega \left[N \|\mathbf{W}_{(\lceil \frac{j}{N} \rceil, :)}^\Omega\| \right] \leq \sqrt{\frac{2}{\pi}} \theta. \quad (56)$$

Combining (56) with (55), we have (53). This finishes the proof.

Condition (3) holds obviously due to the i.i.d assumption of \mathbf{x}_t .

To prove that condition (4) is satisfied, we have

$$\begin{aligned} &\mathbb{E} \left[\left\| \frac{1}{M_t} \sum_{j \in [M_t]} -\nabla \|\mathbf{D}^T \mathbf{y}_t^j\|_3^3 - \nabla F(\mathbf{D}) \right\|_F^2 \right] \\ &\leq \mathbb{E} \left[\left\| \frac{1}{M_t} \sum_{j \in [M_t]} -\nabla \|\mathbf{D}^T \mathbf{y}_t^j\|_3^3 \right\|_F^2 \right] \\ &= \frac{1}{M_t^2} \sum_{j \in [M_t]} \mathbb{E} [\text{trace}((\nabla \|\mathbf{D}^T \mathbf{y}_t^j\|_3^3)^T (\nabla \|\mathbf{D}^T \mathbf{y}_t^j\|_3^3))] \\ &\stackrel{(a)}{\leq} \frac{1}{M_t} \mathbb{E} [\sigma^2(\nabla \|\mathbf{D}^T \mathbf{y}\|_3^3)] \\ &= \frac{1}{M_t} \mathbb{E} [\|(\mathbf{x}^T \mathbf{D}_{true}^T \mathbf{D} \odot |\mathbf{x}^T \mathbf{D}_{true}^T \mathbf{D}|) \mathbf{D}_{true} \mathbf{x}\|_2^2] \\ &\leq \frac{1}{M_t} \mathbb{E} [\| |\mathbf{x}^T \mathbf{D}_{true}^T \mathbf{D}| \odot^2 \mathbf{D}_{true} \mathbf{x} \|_2^2] \\ &\stackrel{(b)}{\leq} \frac{1}{M_t} \sqrt{(\mathbb{E}[\| |\mathbf{x}^T \mathbf{D}_{true}^T \mathbf{D}| \odot^2 \mathbf{D}_{true} \mathbf{x} \|^4])} \sqrt{(\mathbb{E}[\|\mathbf{D}_{true} \mathbf{x}\|_2^4])}, \end{aligned} \quad (57)$$

where (a) is because that matrix $\nabla \|\mathbf{D}^T \mathbf{y}_t^j\|_3^3$ is rank one, (b) is due to the Cauchy-Schwarz inequality. Let $\mathbf{D}_{true}^T \mathbf{D} = \mathbf{W}$, and $\mathbf{W}_{:,i}$ represent the i -th column vector in \mathbf{W} . We have

1)

$$\begin{aligned}
 \mathbb{E}[\|\mathbf{x}^T \mathbf{D}_{true}^T \mathbf{D}^{\odot 2}\|^4] &= \mathbb{E}[\left(\sum_{i=1}^N \|\mathbf{x}^T \mathbf{W}_{:,i}\|^2\right)^2] \\
 &= \mathbb{E}\left[\sum_{i=1}^N \|\mathbf{x}^T \mathbf{W}_{:,i}\|^4\right] + \mathbb{E}\left[\sum_{i' \neq i} \|\mathbf{x}^T \mathbf{W}_{:,i'}\|^2 \|\mathbf{x}^T \mathbf{W}_{:,i}\|^2\right] \\
 &\leq \sum_{i=1}^N \mathbb{E}[\|\mathbf{x}^T \mathbf{W}_{:,i}\|^4] + \sum_{i' \neq i} (\mathbb{E}[\|\mathbf{x}^T \mathbf{W}_{:,i'}\|^4])^{\frac{1}{2}} (\mathbb{E}[\|\mathbf{x}^T \mathbf{W}_{:,i}\|^4])^{\frac{1}{2}} \\
 &\leq \sum_{i=1}^N 3\theta + \sum_{i' \neq i} 3\theta = N^2 3\theta,
 \end{aligned} \tag{58}$$

where the last inequality is according to [26, Lemma B.1].

2) Let $\mathbf{D}_{true(i,:)}$ represent the i -th row vector in \mathbf{D}_{true} .

$$\begin{aligned}
 \mathbb{E}[\|\mathbf{D}_{true(i,:)} \mathbf{x}\|^4] &= \mathbb{E}[\left(\sum_{i=1}^N \|\mathbf{D}_{true(i,:)} \mathbf{x}\|^2\right)^2] \\
 &\leq \sum_{i=1}^N 3\theta + \sum_{i' \neq i} 3\theta = N^2 3\theta.
 \end{aligned} \tag{59}$$

Substituting (58) and (59) into (57) we finish the proof.

REFERENCES

- [1] M. Aharon, M. Elad, and A. Bruckstein, “K-SVD: An algorithm for designing overcomplete dictionaries for sparse representation,” *IEEE Trans. Signal Process.*, vol. 54, no. 11, pp. 4311–4322, 2006.
- [2] J. Mairal, M. Elad, and G. Sapiro, “Sparse representation for color image restoration,” *IEEE Trans. on image processing*, vol. 17, no. 1, pp. 53–69, 2007.
- [3] C. Févotte, N. Bertin, and J.-L. Durrieu, “Nonnegative matrix factorization with the Itakura-Saito divergence: With application to music analysis,” *Neural computation*, vol. 21, no. 3, pp. 793–830, 2009.
- [4] Jianchao Yang, Kai Yu, Yihong Gong, and T. Huang, “Linear spatial pyramid matching using sparse coding for image classification,” in *IEEE Conf. Comput. Vision and Pattern Recognit.*, 2009, pp. 1794–1801.
- [5] J. Wright, A. Y. Yang, A. Ganesh, S. S. Sastry, and Y. Ma, “Robust face recognition via sparse representation,” *IEEE Trans. Pattern Anal. Mach. Intell.*, vol. 31, no. 2, pp. 210–227, 2008.
- [6] S. Mallat, *A Wavelet Tour of Signal Processing*. Elsevier, 1999.
- [7] M. Lustig, D. L. Donoho, J. M. Santos, and J. M. Pauly, “Compressed sensing MRI,” *IEEE Signal Process. Mag.*, vol. 25, no. 2, pp. 72–82, 2008.
- [8] M. Elad and M. Aharon, “Image denoising via sparse and redundant representations over learned dictionaries,” *IEEE Trans. on Image Process.*, vol. 15, no. 12, pp. 3736–3745, 2006.
- [9] I. Ramirez, P. Sprechmann, and G. Sapiro, “Classification and clustering via dictionary learning with structured incoherence and shared features,” in *IEEE Conf. Comput. Vision and Pattern Recognit.*, 2010, pp. 3501–3508.
- [10] K. Engan, S. O. Aase, and J. H. Husoy, “Method of optimal directions for frame design,” in *Proc. IEEE Int. Conf. Acoust. Speech and Signal Process. (ICASSP)*, vol. 5. IEEE, 1999, pp. 2443–2446.
- [11] J. Sun, Q. Qu, and J. Wright, “Complete dictionary recovery over the sphere I: Overview and the geometric picture,” *IEEE Trans. Inf. Theory*, vol. 63, no. 2, pp. 853–884, 2017.
- [12] —, “Complete dictionary recovery over the sphere II: Recovery by riemannian trust-region method,” *IEEE Trans. Inf. Theory*, vol. 63, no. 2, pp. 885–914, 2017.
- [13] Y. Bai, Q. Jiang, and J. Sun, “Subgradient descent learns orthogonal dictionaries,” in *Proc. Int. Conf. Learn. Representations*, 2019.
- [14] Y. Zhai, Z. Yang, Z. Liao, J. Wright, and Y. Ma, “Complete dictionary learning via l4-norm maximization over the orthogonal group,” *J. Machine Learn. Res.*, vol. 21, no. 165, pp. 1–68, 2020.
- [15] P.-A. Absil, R. Mahony, and R. Sepulchre, *Optimization algorithms on matrix manifolds*. Princeton University Press, 2009.
- [16] W. H. Press, S. A. Teukolsky, W. T. Vetterling, and B. P. Flannery, *Numerical recipes 3rd edition: The art of scientific computing*. Cambridge university press, 2007.
- [17] C. Bao, J.-F. Cai, and H. Ji, “Fast sparsity-based orthogonal dictionary learning for image restoration,” in *IEEE Int. Conf. Comput. Vision*, 2013, pp. 3384–3391.
- [18] S. Babu and J. Widom, “Continuous queries over data streams,” *ACM Sigmod Record*, vol. 30, no. 3, pp. 109–120, 2001.
- [19] G. De Francisci Morales, A. Bifet, L. Khan, J. Gama, and W. Fan, “IoT big data stream mining,” in *ACM SIGKDD Int. Conf. Knowl. Discovery and Data Mining*, 2016, pp. 2119–2120.
- [20] A. Bifet and E. Frank, “Sentiment knowledge discovery in twitter streaming data,” in *Int. Conf. on Discovery Science*. Springer, 2010, pp. 1–15.
- [21] R. Johnson and T. Zhang, “Accelerating stochastic gradient descent using predictive reduction,” *Adv. in Neural Inf. Process. Syst.*, vol. 26, pp. 315–323, 2013.
- [22] L. Lei, C. Ju, J. Chen, and M. I. Jordan, “Non-convex finite-sum optimization via SCSG methods,” in *Adv. in Neural Inf. Process. Syst.*, 2017, pp. 2348–2358.
- [23] S. Ghadimi, G. Lan, and H. Zhang, “Mini-batch stochastic approximation methods for nonconvex stochastic composite optimization,” *Math. Program.*, vol. 155, no. 1-2, pp. 267–305, 2016.
- [24] L. Xiao, “Dual averaging methods for regularized stochastic learning and online optimization,” *J. Mach. Learn. Res.*, vol. 11, p. 2543–2596, Dec. 2010.
- [25] Z. Zhou, P. Mertikopoulos, N. Bambos, S. Boyd, and P. W. Glynn, “Stochastic mirror descent in variationally coherent optimization problems,” in *Adv. in Neural Inf. Process. Syst.*, 2017, pp. 7040–7049.
- [26] Y. Shen, Y. Xue, J. Zhang, K. Letaief, and V. Lau, “Complete dictionary learning via ℓ_p -norm maximization,” in

- Proc. Conf. Uncertainty in Artif. Intell. (UAI)*, vol. 124. Virtual: PMLR, 03–06 Aug 2020, pp. 280–289.
- [27] Y. Xue, Y. Shen, V. Lau, J. Zhang, and K. B. Letaief, “Blind data detection in massive MIMO via ℓ_3 -norm maximization over the Stiefel manifold,” *IEEE Trans. on Wireless Commun.*, pp. 1–1, 2020.
- [28] N. Parikh and S. Boyd, “Proximal algorithms,” *Foundations and Trends in optimization*, vol. 1, no. 3, pp. 127–239, 2014.
- [29] S. J Reddi, S. Sra, B. Póczos, and A. J. Smola, “Proximal stochastic methods for nonsmooth nonconvex finite-sum optimization,” *Adv. in Neural Inf. Process. Syst.*, vol. 29, pp. 1145–1153, 2016.
- [30] M. Frank, P. Wolfe *et al.*, “An algorithm for quadratic programming,” *Naval research logistics quarterly*, vol. 3, no. 1-2, pp. 95–110, 1956.
- [31] M. Jaggi, “Revisiting Frank-Wolfe: Projection-free sparse convex optimization,” in *Int. Conf. on Machine Learn.*, 2013, pp. 427–435.
- [32] A. Mokhtari, H. Hassani, and A. Karbasi, “Stochastic conditional gradient methods: From convex minimization to submodular maximization,” *J. Machine Learn. Res.*, vol. 21, no. 105, pp. 1–49, 2020.
- [33] J. Mairal, F. Bach, J. Ponce, and G. Sapiro, “Online dictionary learning for sparse coding,” in *Int. Conf. on Machine Learn.*, 2009, pp. 689–696.
- [34] B. Zhang, N. Mor, J. Kolb, D. S. Chan, K. Lutz, E. Allman, J. Wawrzyniek, E. Lee, and J. Kubiawicz, “The cloud is not enough: Saving IoT from the cloud,” in *7th {USENIX} Workshop on Hot Topics in Cloud Comput. (HotCloud 15)*, 2015.
- [35] T. Lu, W. Xia, X. Zou, and Q. Xia, “Adaptively compressing iot data on the resource-constrained edge,” in *3rd {USENIX} Workshop on Hot Topics in Edge Comput. (HotEdge 20)*, 2020.
- [36] S. P. Kasiviswanathan, P. Melville, A. Banerjee, and V. Sindhwani, “Emerging topic detection using dictionary learning,” in *ACM Int. Conf. on Inf. and Knowl. Manage.*, 2011, pp. 745–754.
- [37] S. Kasiviswanathan, H. Wang, A. Banerjee, and P. Melville, “Online ℓ_1 -dictionary learning with application to novel document detection,” *Adv. in Neural Inf. Process. Syst.*, vol. 25, pp. 2258–2266, 2012.
- [38] C. D. Manning, P. Raghavan, and H. Schütze, *Introduction to Information Retrieval*. USA: Cambridge University Press, 2008.
- [39] Y. Li and Y. Bresler, “Global geometry of multichannel sparse blind deconvolution on the sphere,” in *Proc. Adv. Neural Inf. Process. Syst.*, 2018, pp. 1132–1143.
- [40] Q. Qu, Y. Zhai, X. Li, Y. Zhang, and Z. Zhu, “Geometric analysis of nonconvex optimization landscapes for overcomplete learning,” in *Proc. Int. Conf. Learn. Representations*, 2020.
- [41] M. Journée, Y. Nesterov, P. Richtárik, and R. Sepulchre, “Generalized power method for sparse principal component analysis,” *J. Machine Learn. Res.*, vol. 11, no. Feb, pp. 517–553, 2010.
- [42] E. Hazan and H. Luo, “Variance-reduced and projection-free stochastic optimization,” in *Int. Conf. on Machine Learn.*, ser. Proceedings of Machine Learning Research, M. F. Balcan and K. Q. Weinberger, Eds., vol. 48. New York, New York, USA: PMLR, 20–22 Jun 2016, pp. 1263–1271. [Online]. Available: <http://proceedings.mlr.press/v48/hazana16.html>
- [43] S. J. Reddi, S. Sra, B. Póczos, and A. Smola, “Stochastic frank-wolfe methods for nonconvex optimization,” in *2016 54th Annual Allerton Conference on Communication, Control, and Computing (Allerton)*. IEEE, 2016, pp. 1244–1251.
- [44] J. Duchi, S. Shalev-Shwartz, Y. Singer, and T. Chandra, “Efficient projections onto the ℓ_1 -ball for learning in high dimensions,” in *Int. Conf. on Machine Learn.*, ser. ICML ’08. New York, NY, USA: Association for Computing Machinery, 2008, p. 272–279. [Online]. Available: <https://doi.org/10.1145/1390156.1390191>
- [45] P.-A. Absil and J. Malick, “Projection-like retractions on matrix manifolds,” *SIAM J. on Optim.*, vol. 22, no. 1, pp. 135–158, 2012.
- [46] Airly, “Air quality data from extensive network of sensors: PM1, PM2.5, PM10, temp, pres and hum data for 2017 year from Krakow, Poland.” [Online]. Available: <https://www.kaggle.com/datascienceairly/air-quality-data-from-extensive-network-of-sensors>
- [47] W. H. Young, “On classes of summable functions and their fourier series,” *Proceedings of the Royal Society of London. Series A, Containing Papers of a Mathematical and Physical Character*, vol. 87, no. 594, pp. 225–229, 1912.
- [48] A. Mokhtari, H. Hassani, and A. Karbasi, “Conditional gradient method for stochastic submodular maximization: Closing the gap,” in *Int. Conf. on Artificial Intell. and Statistics*, ser. Proceedings of Machine Learning Research, A. Storkey and F. Perez-Cruz, Eds., vol. 84. PMLR, 09–11 Apr 2018, pp. 1886–1895.